https://doi.org/10.5194/egusphere-2025-1909
Preprint. Discussion started: 15 May 2025


# Pathway-specific responses of isoprene-derived secondary organic aerosol formation to anthropogenic emission reductions in a megacity in eastern China

Huilin Hu[1], Yunyi Liang[2], Ting Li[2], Yongliang She[2], Yao Wang[1,3], Ting Yang[1], Min Zhou[4], Ziyue Li[1], Chenxi Li[1], Huayun Xiao[1], Jianlin Hu[2], Jingyi Li[2,*], Yue Zhao[1,*]

[1]School of Environmental Science and Engineering, Shanghai Jiao Tong University, Shanghai 200240, China

[2]Jiangsu Key Laboratory of Atmospheric Environment Monitoring and Pollution Control, Collaborative Innovation Center of Atmospheric Environment and Equipment Technology, School of Environmental Science and Engineering, Nanjing University of Information Science and Technology, Nanjing 210044, China

[3]Ningbo Ecological and Environmental Monitoring Center, Ningbo 315012, China,

[4]State Environmental Protection Key Laboratory of the Cause and Prevention of Urban Air Pollution Complex, Shanghai Academy of Environmental Sciences, Shanghai 200233, China

Correspondence: Yue Zhao (yuezhao20@sjtu.edu.cn); Jingyi Li (Jingyili@nuist.edu.cn)

https://doi.org/10.5194/egusphere-2025-1909
Preprint. Discussion started: 15 May 2025


**ABSTRACT：** Isoprene-derived secondary organic aerosol (iSOA) represents a major biogenic source of atmospheric OA and its formation is profoundly influenced by anthropogenic emissions. However, long-term iSOA measurements in polluted urban regions remain limited, hindering the understanding of anthropogenic influences on iSOA formation. In this study, field observations of iSOA were conducted in Shanghai, China during summers and winters of 2015, 2019, and 2021, aiming to assess the iSOA response to emission reductions over this period. The particulate iSOA tracers formed via reactive uptake of isoprene epoxydiol (IEPOX), a hydroperoxy radical-dominated pathway, and hydroxymethylmethyl-α-lactone (HMML) and/or methacrylic acid epoxide (MAE), a $NO_x$-dominated pathway, were measured by mass spectrometry. Both total and IEPOX-derived iSOA decreased markedly from 2015 to 2021, while summertime HMML/MAE-SOA did not vary significantly despite strong NOx reductions. Declining aerosol reactivity toward IEPOX/HMML/MAE and reduced atmospheric oxidizing capacity drove the decrease in IEPOX-SOA but could not explain the trend of summertime HMML/MAE-SOA. Simulations of iSOA with the Community Multiscale Air Quality model in 2015 and 2019 captured the decreasing IEPOX-SOA trend and confirmed a driving role of chemical processes. However, the model failed to replicate relatively stable HMML/MAE-SOA levels in summer, suggesting additional factors (e.g., the potential unaccounted sources of methacrolein, the precursor to HMML/MAE) may buffer HMML/MAE-SOA variations. These findings demonstrate the pathway-specific iSOA responses to emission reductions in a megacity and emphasize the importance of regulating atmospheric oxidizing capacity and aerosol reactivity to mitigate biogenic SOA formation in urban environments.

https://doi.org/10.5194/egusphere-2025-1909
Preprint. Discussion started: 15 May 2025


## 1. Introduction

Isoprene (2-methyl-1,3-butadiene, $C_5H_8$), mainly emitted by terrestrial vegetation, represents the largest source of atmospheric non-methane hydrocarbons, with a global emission flux of 500-750 Tg $yr^{-1}$ (Guenther et al., 2006). Because of its large abundance and high reactivity, the oxidation of isoprene contributes significantly to the formation of secondary organic aerosol (SOA) in the troposphere, estimated to 19.2 TgC $yr^{-1}$ (Heald et al., 2008). The formation chemistry of iSOA has been extensively studied in laboratory, field, and modelling studies, which have shown that anthropogenic pollutants such as nitrogen oxides ($NO_x$) and sulfur dioxide ($SO_2$, the precursor to particulate sulfate) play a crucial role in the formation of iSOA (Shrivastava et al., 2019).

Photooxidation is the dominant fate of isoprene in the atmosphere, during which the C=C bond of isoprene is initially attacked by OH radicals to produce an alkyl radical (Teng et al., 2017), followed by the formation of isoprene hydroxyperoxy radicals ($ISOPO_2$) via oxygen addition (Surratt et al., 2010). The fate of $ISOPO_2$ radicals depends on the environmental conditions. When the $NO_x$ level is sufficiently low (referred to as $HO_2$-dominated conditions), $ISOPO_2$ would mainly react with $HO_2$ radicals to form hydroxyhydroperoxides (ISOPOOH) (Paulot et al., 2009). Further OH radical addition to ISOPOOH produces isomeric isoprene epoxydiols (IEPOX, trans-β-IEPOX: cis-β-IEPOX = 0.63:0.37) with a yield of ~70-80% (Paulot et al., 2009; Bates et al., 2014; St. Clair et al., 2016). The gaseous IEPOX can be taken up into aqueous aerosol and undergo acid-catalyzed reactions to form polyols, organosulfates (OSs), and oligomers. Several constituents including 2-methyltetrols (2-MT) and their oligomers, $C_5$-alkene triols, methyl tetrahydrofurans, and 2-methyltetrol sulfates (2-MT-OS), which were abundantly measured in both laboratory-generated and ambient SOA (Xu et al., 2015; Isaacman-Vanwertz et al., 2016; Surratt et al., 2010; Surratt et al., 2007; Worton et al., 2013; Yee et al., 2020), have been employed as molecular tracers of SOA derived from reactive uptake of IEPOX (IEPOX-SOA).

When the $NO_x$ level is high (referred to as NOx-dominated conditions), $ISOPO_2$ would preferentially react with NO, producing unsaturated carbonyls such as methacrolein (MACR) and methyl vinyl ketone (MVK). A large fraction (□45%) of MACR can be further oxidized by OH radicals via aldehydic H-abstraction, followed by oxygen addition to form an acylperoxy radical, $MACRO_2$

https://doi.org/10.5194/egusphere-2025-1909
Preprint. Discussion started: 15 May 2025


(Orlando et al., 1999). Subsequent reaction between $MACRO_2$ and $NO_2$ yields MPAN, which was proposed to form hydroxymethyl methyl-α-lactone (HMML) or methacrylic acid epoxide (MAE) (Nguyen et al., 2015; Lin et al., 2013b). Both of these two epoxides can undergo heterogeneous acid-catalyzed reactions to form 2-methylglyceric acid (2-MG) as well as its oligoesters and sulfated derivatives (2-methylglyceric acid sulfate, 2-MG-OS), which serve as the molecular tracers of HMML/MAE-derived SOA (Kjaergaard et al., 2012; Lin et al., 2013b).

In addition to altering the fate of $RO_2$ (including $ISOPO_2$ and $MACRO_2$), $NO_x$ also plays an essential role in regulating atmospheric oxidizing capacity (e.g., the OH level), which governs the photooxidation rate of isoprene in the atmosphere. Compared to NOx that strongly affect the gas-phase oxidation chemistry of isoprene, sulfate aerosol mainly exerts influences on the multiphase chemistry of isoprene-derived epoxides. On one hand, sulfate serves as an important nucleophile in the reactive uptake of isoprene epoxides to form OSs, which competes with the reaction of epoxides with water (Lin et al., 2013b). On the other hand, sulfate can alter the physicochemical properties of particles such as liquid water content (LWC), acidity, and phase state (Zhao et al., 2018; Zhao et al., 2019; Ye et al., 2018), which are the key factors influencing the multiphase reactivity of epoxides and the formation of iSOA.

Because of the complexity in the gas-phase and multiphase chemistry leading to iSOA formation, the product distribution of $HO_2$- versus $NO_x$-dominated pathways as well as their dependence on different influencing factors (i.e., NOx, sulfate, LWC, and aerosol acidity) varies significantly in different environments. A number of field measurements have found that the formation of IEPOX-SOA tracers was predominated over the HMML/MAE-SOA tracers, even in some $NO_x$-rich urban areas (Zhang et al., 2022; Hu et al., 2008; Yee et al., 2020), while a few studies showed that the production of HMML/MAE-SOA was more prevalent, e.g., in Tianjin, China (Fan et al., 2020) and urban areas of California (Lewandowski et al., 2013). Sulfate was found to be the primary driver of isoprene-derived SOA in rural and urban regions as the iSOA correlated strongly with sulfate while such correlation did not occur with LWC and pH, e.g., in central Amazonia and southeastern U.S (Xu et al., 2015; Yee et al., 2020). It should be noted that significant uncertainties exist in the quantification of iSOA tracers in ambient aerosols due to the lack of authentic standards and/or the presence of measurement artifacts

https://doi.org/10.5194/egusphere-2025-1909
Preprint. Discussion started: 15 May 2025


(e.g., matrix effects) (Fu et al., 2012; Wang et al., 2008; Ding et al., 2014; Fu et al., 2016; Fu et al., 2014; Fan et al., 2020; Zhong et al., 2021). Furthermore, previous studies have mainly focused on the characterization of the particle-phase abundance of the iSOA tracers (Zhang et al., 2022; Zhang et al., 2019; Kang et al., 2018). Given that the iSOA tracers can actively partition between gas and particle phases, considering their particle-phase concentration only may significantly bias our understanding of the atmospheric abundance and chemistry of iSOA (Nguyen et al., 2015; Fan et al., 2020; Isaacman-Vanwertz et al., 2016). As a result, there remain large uncertainties in identifying the anthropogenic influence on iSOA formation in ambient air.

In recent years, great changes have taken place in air pollutant emissions, atmospheric composition, and air quality in China due to the implementation of stringent clean air policies nationwide. For example, $PM_{2.5}$ mass concentrations dropped significantly, with a notable reduction in inorganic water-soluble ions such as sulfate, ammonium, and cation ions (Liu et al., 2023a; Zheng et al., 2018; Zhao et al., 2015; Huang et al., 2014; Liu et al., 2023b), and a relatively small decrease in organic aerosol in eastern China in the past decade (Liu et al., 2023a; Yao et al., 2023). The reduction of inorganic ions including sulfate and non-volatile cations ($Na^+$, $K^+$, $Ca^{2+}$ and $Mg^{2+}$) resulted in a significant decrease in LWC and a slight increase in aerosol acidity in this region (Zhou et al., 2022). However, concentrations of VOCs and ozone exhibited different trends, with a slight decrease for the former while the later showing an upward trend before 2018 and a slight declining trend after 2018 (Wang et al., 2022; Liu et al., 2023a; Yao et al., 2023; Gong et al., 2025). The changing atmospheric conditions can affect both gas-phase and particle-phase chemistry, as well as the gas-particle partitioning behavior of organics. However, how the formation of biogenic SOA, such as iSOA, respond to the changes in anthropogenic emissions and air pollution conditions in polluted regions remains poorly understood.

The aim of this study is to comprehend the atmospheric abundance and formation mechanisms of iSOA under the influence of continuous anthropogenic emission reductions in eastern China. Ambient $PM_{2.5}$ samples were collected at an urban site in megacity Shanghai in winter and summer of 2015, 2019, and 2021. The concentrations of isoprene-derived polyols and OSs from both $HO_2$- and $NO_x$-dominated pathways in $PM_{2.5}$ samples were measured using gas chromatography-mass spectrometry (GC-MS) and high-resolution liquid chromatography-mass spectrometry (LC-MS), respectively, with

https://doi.org/10.5194/egusphere-2025-1909
Preprint. Discussion started: 15 May 2025


the aid of a suite of authentic and surrogate standards. The quantification errors of iSOA tracers were evaluated and their gas-particle partitioning behaviors were considered. The relative distribution of measured iSOA tracers from different pathways as well as their inter-annual and seasonal variations were analyzed and compared to the calculated reaction efficiency of different pathways as well as the simulated values using the Community Multiscale Air Quality (CMAQ) model, which helps to constrain the formation mechanisms of iSOA and the key factors driving the inter-annual variation of iSOA tracers.

## 2. Materials and methods

### 2.1 Sampling and Chemical Analysis

Ambient $PM_{2.5}$ samples were collected on the rooftop of a 20-m tall teaching building at Xuhui Campus of Shanghai Jiao Tong University (31.201° N, 121.429° E) located in the urban center of Shanghai, China. The site is impacted by a mixed commercial and residential area. The sampling campaigns were conducted in summer (July 14 to August 9 in 2015; 14 July to 9 August 2019; 7 July to 5 August 2021) and winter (6 January to 26 January 2016; 27 December 2018 to 16 January 2019; 22 December 2021 to 18 January 2022) of 2015, 2019, and 2021. Sampling started at 8:00 am local time and lasted for 23 hours. A total of 138 $PM_{2.5}$ samples were collected on prebaked (550 ℃, 6 h) quartz filters (18 × 23 $cm^2$, Whatman) using a high-volume sampler (HiVol 3000, Ecotech) at a flow rate of 67.8 $m^3$ $h^{-1}$. All sampled filters were wrapped with prebaked aluminum foil and stored at -20 ℃ until analysis.

iSOA polyol tracers, included 2-MG, cis-2-methyl-1,3,4-trihydroxy-1-butene, trans-2-methyl-1,3,4-trihydroxy-1-butene, and 3-methyl-2,3,4-trihydroxy-1-butene (cis-2-MTB, trans-2-MTB, and 3-MTB, collectively named as $C_5$-alkene triols), as well as 2-methylthreitol and 2-methylerythritol (collectively named as 2-MTs), were analyzed by a GC-MS. The details regarding the sample preparation and analysis protocol are presented in Section S1 in the supplement. An example of the total ion chromatograms (TIC) of iSOA polyol tracers is shown in Figure S1d. For iSOA polyol tracers, surrogate standards including erythritol, KPA, and glycerol were used for quantifications in a number of studies (Kang et al., 2018; Ding et al., 2014; Zhang et al., 2019; Fan et al., 2020). In this study, concentrations of 2-MG and 2-methylerythritol were quantified using their authentic standards, and $C_5$-alkene triols and 2-methylthreitol were quantified by 2-methylerythritol. The uncertainty for $C_5$-alkene

https://doi.org/10.5194/egusphere-2025-1909
Preprint. Discussion started: 15 May 2025


triols was estimated previously and their concentration was found to be underestimated by 65% when 2-methylerythritol was used as the surrogate standard (Frauenheim et al., 2022). Furthermore, the uncertainty of 2-methylthreitol quantified by 2-methylerythritol was assumed to be negligible as the differences in the TIC response for homologues are determined by carbon number, functional groups, and number of active hydrogen atoms that would silylate (Stone et al., 2012).

The particulate iSOA OSs were analyzed by a LC-MS employing a reversed-phase column ($C_{18}$, 2.1 mm ×100 mm, 1.7 μm, Waters). The sample extraction procedure and analysis protocol were described in detail in our previous work (Wang et al., 2021). A brief summary is given in Section S2 and examples of total and extracted ion chromatograms of iSOA OSs are provided in Figure S1a-c. The lactic acid sulfate (LAS) was used as a surrogate standard to quantify the 2-MT-OS and 2-MG-OS. Previous studies illustrated that the ESI efficiency is dependent on structures of species (Kebarle, 2000). More relevantly, Bryant et al.(Bryant et al., 2021) showed that camphorsulfonic acid (CAS), another commonly used surrogate standard for the quantification of 2-MT-OS and 2-MG-OS (Wang et al., 2023b; He et al., 2014; Hettiyadura et al., 2015), is ionized 2.4 times more efficiently than 2-MT-OS and 12.4 times more than 2-MG-OS. In this study, the relative ionization efficiency of CAS vs. LAS was measured to estimate the quantification uncertainties of iSOA OSs, based on the reported relative ionization efficiency of CAS vs. iSOA OSs (Bryant et al., 2021). Our results showed that the CAS ionized 4.62 times more efficiently than LAS. Accordingly, LAS would ionize 1.9 times less efficiently than 2-MT-OS and 2.68 times more than 2-MG-OS. This suggests that the concentration of 2-MT-OS might be 48% lower than quantified using LAS, while that of 2-MG-OS was 168% higher than quantified by LAS.

### 2.2 Additional measurements and models

The concentrations of organic carbon (OC) and element carbon (EC) in filter samples were measured using a thermal–optical multiwavelength carbon analyzer (DRI, Model 2015). The concentration of organic mass (OM) was estimated by multiplying the OC by 1.6 (Tao et al., 2014). An ion chromatograph (Metrohm MIC) was employed to determine water-soluble inorganic compounds (e.g., sulfate, nitrate, chloride, ammonium, potassium ion, and calcium ion). Temperature, relative humidity (RH), as well as the concentrations of trace gases and $PM_{2.5}$ were measured at a meteorological

https://doi.org/10.5194/egusphere-2025-1909
Preprint. Discussion started: 15 May 2025


station and an air quality monitoring station several km away from the sampling site. The details of the two stations were described in our previous study (Wang et al., 2021) and the mean values of these meteorological parameters and pollutant concentrations are listed in Table S1.

LWC, pH, and bisulfate concentration in aqueous aerosols were predicted by the ISORROPIA-II thermodynamic model (Wang et al., 2021). The molar concentrations of particulate water-soluble inorganic ions (including sulfate, nitrate, chloride, ammonium, potassium ion, and calcium ion), temperature, and RH were input into the model, which was run in the forward mode for metastable aerosols. As the predicted aerosol pH could be underestimated when using particle-phase concentrations of ion species as inputs only (Hennigan et al., 2015), we adopted the pH values of 2015 and 2019 at a nearby site reported by Zhou et al. (2022), who used both particulate inorganic ion concentrations and gaseous ammonia as inputs of ISORROPIA-II. Additionally, by comparing the predicted pH values of 2015 and 2019 in this study with the reported values in Zhou et al. (2022) during the same observation period, we found that the aerosol pH predicted using gas + aerosol inputs was on average one unit larger than that using aerosol inputs only. Therefore, output pH values of 2021 in this study were increased by one unit to represent the aerosol acidity.

In addition, considering that iSOA polyol tracers are semi-volatile and water-soluble, which can partition into OM or dissolve into aerosol liquid water, their gas-phase and particle-phase fractions were estimated by accounting for the gas-organic phase partitioning using an organic absorptive equilibrium partitioning model and the gas-aqueous phase partitioning using the Henry's Law. The details of the estimation method are described in Section S3.

### 2.3 Quality control and quality assurance

Procedural blanks (run every 6 samples) and field blanks (two for each season) were extracted and analyzed in the same manner as the $PM_{2.5}$ filter samples. Target compounds were found below the detection limit in the blanks. The recovery of iSOA polyol tracers as represented by that of the internal standard (ketopinic acid) during GC-MS analysis was determined to be 85±17% and the recovery of iSOA OSs during LC-MS analysis was 72.5%, as determined using LAS spiked onto the filter in our previous study (Wang et al., 2021).

https://doi.org/10.5194/egusphere-2025-1909
Preprint. Discussion started: 15 May 2025


As the $PM_{2.5}$ sample extracts contain thousands of multifunctional compounds, there might exist a significant matrix effect in the analysis of iSOA tracers. The matrix effect of polyol tracers was evaluated by comparing the signal responses of authentic standards of 2-methylerythritol and 2-MG in $PM_{2.5}$ extracts to those in pure solvent. Six filter samples representing low and high $PM_{2.5}$ concentrations in summer and winter were used to test the matrix effect. 16 μL or 160 μL of 2-methylerythritol and 2-MG standard mixtures (10 ppm) was added to the filter extracts to represent the low and high concentrations of 2-methylerythritol and 2-MG in the samples. The filters were subsequently analyzed as described in Section 2.2. The matrix factors of the standards were calculated as the ratio of their signal response in sample extracts (the signal response of these species in non-spiked extracts was subtracted) to their signal response in the pure solvent. As shown in Table S2, 2-MG had a matrix factor of 0.77 ± 0.12, while that of 2-methylerythritol was 1.24 ± 0.08, indicating that the concentrations of 2-MG were likely underestimated by 23% whereas 2-methylerythritol was overestimated by 24% due to the matrix effect.

For OS tracers, Bryant et al. (2021) have assessed the matrix effect of 2-MT-OS and 2-MG-OS using authentic standards and found that the matrix factors were 0.29 ± 0.23 and 0.84 ± 0.18, respectively. If similar matrix effects for 2-MT-OS and 2-MG-OS reported by Bryant et al. (2021) occurred in our measurements, the concentrations of these two OS species would be underestimated by 71% and 16%, respectively.

### 2.4 Estimation of the reaction efficiency of isoprene-derived epoxides in aqueous aerosols

The IEPOX/HMML/MAE can undergo acid-catalyzed nucleophilic addition with water and sulfate to form polyol tracers (2-MTs and 2-MG) and OSs (2-MT-OS and 2-MG-OS) in aqueous aerosols, respectively. The aqueous-phase pseudo-first-order rate constants ($k_{aq}$, $s^{-1}$) for epoxides could be estimated by eq 1 (Eddingsaas et al., 2010),

$$k_{aq} = \sum_{i=1}^{N} \sum_{j=1}^{M} k_{ij} [nuc_i]_{aq} [acid_j]_{aq} \quad (1)$$

Where $k_{ij}$ is the third-order reaction rate constant of isoprene-derived epoxides with nucleophile i (water or sulfate) and acid j (hydrogen ion or bisulfate) in the aqueous phase and the reported values of

https://doi.org/10.5194/egusphere-2025-1909
Preprint. Discussion started: 15 May 2025


$k_{ij}$ in previous studies are shown in Table 1. When epoxides react with water and sulfate, the aqueous-phase reaction rate constants ($k_{aq,\ H_2O}$ and $k_{aq,\ SO_4^{2-}}$) can be estimated by eqs 2 and 3, respectively.

$$k_{aq,\ H_2O}=k_{H_2O,H^+}[H_2O]_{aq}[H^+]_{aq}+k_{H_2O,HSO_4^-}[H_2O]_{aq}[HSO_4^-]_{aq} \quad (2)$$

$$k_{aq,\ SO_4^{2-}}=k_{SO_4^{2-},H^+}[SO_4^{2-}]_{aq}[H^+]_{aq}+k_{SO_4^{2-},HSO_4^-}[SO_4^{2-}]_{aq}[HSO_4^-]_{aq} \quad (3)$$

Where $[H^+]_{aq}$, $[HSO_4^-]_{aq}$, and $[H_2O]_{aq}$ are molar concentrations of hydrogen ion, bisulfate, and ALWC in aqueous aerosols, which were estimated by ISORROPIA-II model, and $[SO_4^{2-}]_{aq}$ is the molar concentration of sulfate.

The reactive uptake coefficient (γ) of epoxides on aqueous aerosols is parameterized by a resistor model (Xu et al., 2016; Pye et al., 2013).

$$\frac{1}{\gamma}=\frac{1}{\alpha}+\frac{\omega}{4H_{epoxide}RT\sqrt{D_a k_{aq}}}\frac{1}{f(q)} \quad (4)$$

$$f(q)=\coth(q)-\frac{1}{q} \quad (5)$$

$$q=r_p\sqrt{k_{aq}/D_a} \quad (6)$$

Where $r_p$ is the particle radius. Previous work has found that the surface area ($S_a$, $m^2\ m^{-3}$) and volume concentrations ($V_a$, $m^3\ m^{-3}$) of dry $PM_{2.5}$ could be described as a function of $PM_{2.5}$ mass concentration ($C_{PM_{2.5}}$, μg $m^{-3}$) in Shanghai ($S_a=7.54\times10^{-6}\bullet C_{PM_{2.5}}+1.01\times10^{-4}$, $V_a=5.59\times10^{-13}\bullet C_{PM_{2.5}}+1.02\times10^{-12}$) (Zang et al., 2022). In this study, the mean particle radius of dry $PM_{2.5}$ was calculated as $3V_a/S_a$, which was then corrected for the aerosol hygroscopic growth to get the wet particle radius based on the κ-Köhler hygroscopicity function (see details in Section S4). α is the mass accommodation coefficient taking a value of 0.02 for both IEPOX and HMML/MAE (Mcneill et al., 2012), ω is the mean molecular velocity of epoxides, $H_{epoxide}$ is the Henry's law constant in the aqueous phase, with a value of $2.7\times10^6$ M $atm^{-1}$ for IEPOX (Pye et al., 2013) and a constrained value of $7.5\times10^6$ M $atm^{-1}$ for HMML/MAE by CMAQ in Case 1, and $k_{aq}$ is the first-order reaction rate constant in the aqueous phase ($s^{-1}$), estimated using eq 1.

https://doi.org/10.5194/egusphere-2025-1909
Preprint. Discussion started: 15 May 2025


To describe the overall loss rate of gas-phase epoxides due to the reactive uptake by aqueous aerosols, the pseudo-first-order heterogeneous reaction rate constant was calculated by eq 7, when neglecting the gas-phase diffusion limitation:

$$k_{het} = \gamma \omega S_a / 4 \quad (7)$$

**2.5 Model Simulations**

The CMAQ model (v5.2) was adopted to simulate the gas-phase concentration of isoprene and particulate concentrations of 2-MTs, 2-MG, and their OS derivatives formed involving the reactive uptake of IEPOX and HMML/MAE on aqueous aerosols (Pye et al., 2017) in both summer and winter of 2015 and 2019 in Shanghai. The simulations performed with the standard CMAQ v5.2 are referred to as the Base Case. While the advanced model simulations performed according to a recent study by Zhang et al. (2023) are named as Case 1. In this advanced case, the iSOA polyol tracers were treated as semi-volatile species that partition between gas, aqueous, and organic phases, while the OS tracers were treated as non-volatile species. The removal of iSOA polyol tracers by OH radicals in the gas and particle phases was also considered. The key parameters for simulating reactive uptake of IEPOX/HMML/MAE and the removal of 2-MT and 2-MG in the gas phase and aqueous aerosol in the model are listed in Table S3 and S4.

In this work, three nested domains covering mainland China, eastern China, and the Yangtze River Delta were configured with horizontal resolutions of 36 km × 36 km (d01), 12 km × 12 km (d02), and 4 km × 4 km (d03), as shown in Figure S2. The outermost domain (d01) was driven by predefined initial and boundary conditions from CMAQ, with its outputs supplying these conditions for d02, which in turn provided them for d03. All domains employed a vertical structure consisting of 18 layers, extending from the surface to an altitude of 21 km.

Anthropogenic emissions were sourced from the Multi-resolution Emission Inventory for China (MEIC) version 1.4 for China (Geng et al., 2024) and the Regional Emission inventory in ASia (REAS) version 3.2.1 for other Asian countries and regions (Kurokawa and Ohara, 2020). Open biomass burning emissions were based on the Fire INventory from NCAR (FINN) version 2.5 (Wiedinmyer et al., 2023). Biogenic emissions were estimated using the Model of Emissions of Gases and Aerosols from Nature (MEGAN) version 2.1, incorporating the high-quality Leaf Area Index (HiQ-LAI) dataset

https://doi.org/10.5194/egusphere-2025-1909
Preprint. Discussion started: 15 May 2025


developed by Yan et al. (2024), which enhances the spatiotemporal consistency of MODIS LAI products. Meteorology data was generated by the Weather Research and Forecasting (WRF) model version 4.2.1 with initial and boundary conditions from the fifth generation ECMWF atmospheric reanalysis data (ERA5).

The simulation was conducted for four periods: 12 July–9 August 2015, 25 December 2015–16 January 2016, 4–26 January 2019, and 12 July–5 August 2019. The first two days of each period were treated as spin-up periods and excluded from the analysis.

## 3. Results and Discussion

### 3.1 Temporal evolution of major air pollutants during the observation period

Time series of $PM_{2.5}$ and its major components, as well as the major trace gases ($NO_2$ and $O_3$) and meteorological parameters during the observation period are shown in Figure 1 and their seasonally averaged values are presented in Table S1. The concentration of $NO_2$ exhibited an obvious downward trend, in particular in summer from 2015 to 2021, consistent with a strong reduction in anthropogenic emissions during this period. By contrast, $O_3$ showed a more complex inter-annual trend, with the average concentration dropped from 52.0 ± 38.9 ppb in 2015 to 41.2 ± 22.8 ppb in 2019, but then increased to 43.4 ± 20.8 ppb in 2021, suggesting a complex response of secondary $O_3$ formation to primary emission reductions. During the observation period, the concentrations of $PM_{2.5}$, most of the inorganic ions (sulfate, chloride, and ammonium), and OM exhibited a dramatic descending trend in both seasons (see Table S1). In contrast, the concentration of aerosol nitrate showed a slight upward trend during this period, in line with the measurement in urban Shanghai by Zhou et al. (2022). Overall, OM was the most abundant component in $PM_{2.5}$, accounting for 10.2-72.7% of total $PM_{2.5}$ mass, followed by sulfate (6.8-45.2%), nitrate (0.5-32.6%), and ammonium (1.1-18.2%). Ascribed to the strong decrease of inorganic ion concentrations (in particular sulfate), aerosol LWC decreased dramatically from 2015 to 2021. Aerosol pH decreased from 3.2 ± 0.4 in 2015 to 2.5 ± 0.9 in 2021, which was mainly driven by the decrease of non-volatile cations during these years, though the decreased concentrations of sulfate had an opposite effect on aerosol acidity (Zhou et al., 2022).

https://doi.org/10.5194/egusphere-2025-1909
Preprint. Discussion started: 15 May 2025


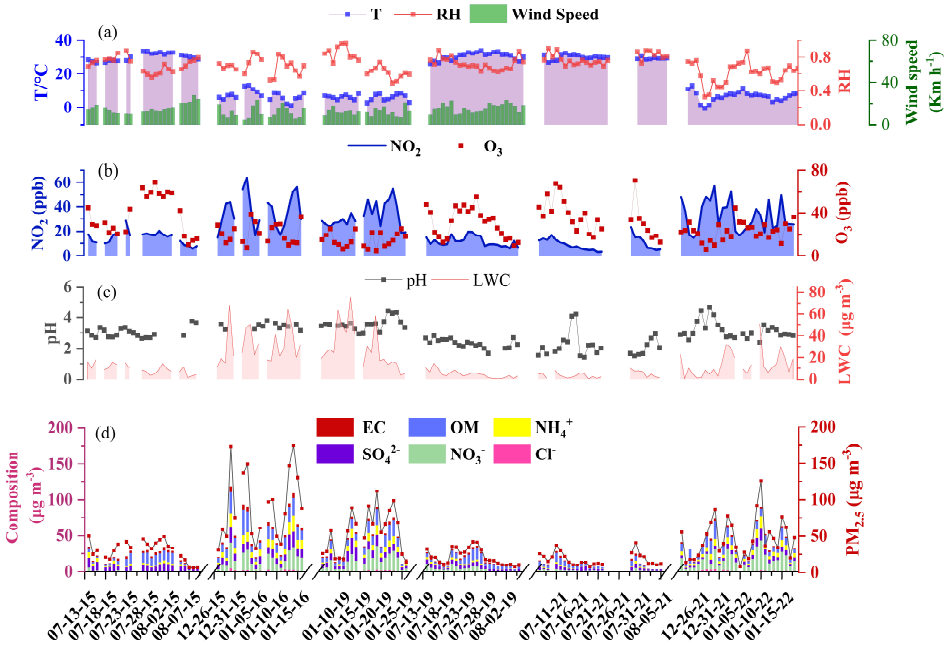


Figure 1. Temporal variations of (a) meteorological parameters (ambient temperature, relative humidity, and wind speed), (b) concentrations of $NO_2$ and $O_3$, (c) aerosol pH and liquid water content (LWC), and (d) concentrations of $PM_{2.5}$ and its major components (OM, EC, sulfate, nitrate, chloride, and ammonium) in urban Shanghai during the observation period.

### 3.2 Seasonal and annual variations of iSOA tracers

The measured concentrations of particulate iSOA tracers during the observation period are summarized in Figure 2 and their specific concentration values are also provided in Table S1. Among the measured iSOA tracers, $C_5$-alkene triols were the most abundant species with average concentrations of 27.6 ng $m^{-3}$ in 2015, 20.9 ng $m^{-3}$ in 2019, and 11.1 ng $m^{-3}$ in 2021, accounting for 28.8 %, 22.4, and 18.7 % of the total iSOA mass, followed by 2-MT-OS, 2-MTs, 2-MG-OS, and 2-MG. The particulate concentrations of IEPOX-SOA (94.1, 82.3, and 51.7 ng $m^{-3}$ in 2015, 2019 and 2021, respectively) dominated over HMML/MAE-SOA (6.2, 6.4, and 7.7 ng $m^{-3}$) in summer, while the concentrations of IEPOX-SOA were slightly lower than HMML/MAE-SOA in winter. The dominance of IEPOX-SOA over HMML/MAE-SOA in summer is in agreement with field studies conducted in Beijing, Hefei and Kunming in China (Zhang et al., 2022) and Southeastern US (Budisulistiorini et al., 2015; Rattanavaraha et al., 2016; Lin et al., 2013a).

https://doi.org/10.5194/egusphere-2025-1909
Preprint. Discussion started: 15 May 2025


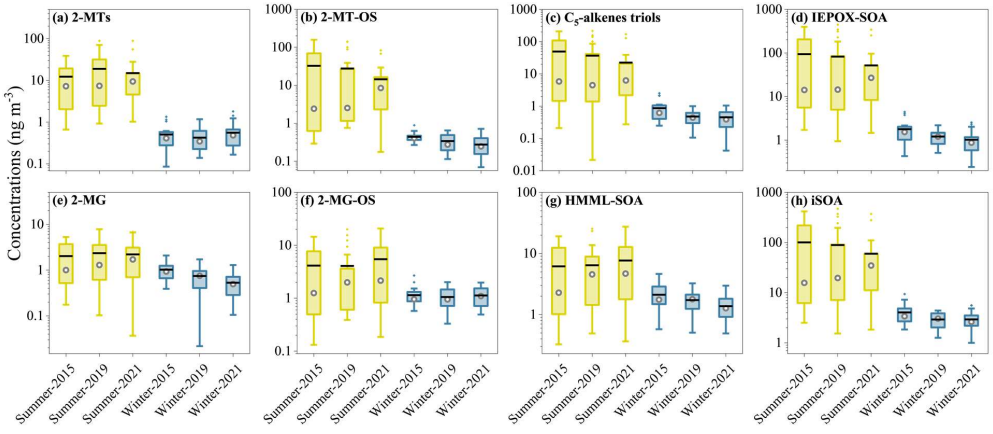


Figure 2. Seasonal and inter-annual variations in particulate concentrations of (a) 2-MTs, (b) 2-MT-OS, (c) $C_5$-alkene triols, (d) IEPOX-SOA (the sum of 2-MTs, 2-MT-OS, and $C_5$-alkene triols), (e) 2-MG, (f) 2-MG-OS, (g) HMML/MAE-SOA (2-MG plus 2-MG-OS), and (h) iSOA (the sum of all tracers).

The annual average particulate concentration of the total iSOA polyol tracers (including 2-MTs, 2-MG, and $C_5$-alkene triols) were 36.1, 33.4, and 18.7 ng $m^{-3}$ in 2015, 2019 and 2021, higher than those of OS tracers (including 2-MT-OS and 2-MG-OS) by a factor of 2.5, 2.1, and 1.4, respectively. The dominance of iSOA polyol tracers over OS tracers is in agreement with observations in other urban regions (Zhang et al., 2022; He et al., 2018).

The particle-phase concentrations of total and specific IEPOX-SOA tracers (except 2-MTs) decreased yearly in both summer and winter between 2015-2021 (Figs. 2a-d), while the particulate concentrations of total and specific HMML/MAE-SOA species did not show a significant inter-annual trend in summer during this period (Figs. 2e-g). 2-MTs exhibited a different inter-annual trend compared to other IEPOX-SOA tracers. A possible explanation for this discrepancy is that 2-MTs may have origins other than reactive uptake of IEPOX on aqueous aerosol. Previous studies have found that 2-methylerythritol, one isomer of 2-MTs, could be generated by biosynthetic pathways (Duvold et al., 1997; Sagner et al., 1998; Rohmer, 1999; Lange et al., 2000; Yang et al., 2013). And the contributions of non-IEPOX pathway to 2-MTs concentrations were pH-dependent, accounting for 20-40% in areas with aerosol pH < 2 and more than 70% under less acidic conditions (pH ~ 2–5) (Zhang et al., 2023). The contribution of biological emissions to 2-MTs might be important in Shanghai given its less acidic

https://doi.org/10.5194/egusphere-2025-1909
Preprint. Discussion started: 15 May 2025


aerosol conditions (pH > 2). As a whole, the particulate concentrations of iSOA decreased significantly in both seasons from 2015 to 2021. In addition, all iSOA compound classes had substantially higher concentrations in summer than in winter. Such a strong seasonality in abundance is mainly driven by the higher temperature and stronger solar radiation, and thereby more intensive isoprene emissions and photochemistry in summer than in winter. Notably, HMML/MAE-SOA species exhibited a relatively smaller seasonal variation than IEPOX-SOA. This is partially owing to the fast thermolysis of methacryloyl peroxynitrate (MPAN) in summer, reducing the formation of HMML/MAE and thereby SOA (Worton et al., 2013).

To further investigate factors that affect the abundance of iSOA, the particulate concentrations of 2-MTs, 2-MT-OS, 2-MG, and 2-MG-OS, as well as the gas-phase concentration of isoprene were simulated with the CMAQ model and compared to measurements in summertime and wintertime of 2015 and 2019 (see Figure 3). Predicted concentrations of isoprene were generally consistent with observations with a median correlation ($r^2$=0.45), except in the summer of 2015, during which isoprene concentrations were significantly overestimated (Figure 3a). For iSOA tracers, the Case 1 showed a better prediction with the observed concentrations than the Base Case. Overall, the simulated IEPOX-SOA tracers were biased low in summer, but biased high in winter (Figure 3b and 3c), though the isoprene precursor was overestimated more in summer than in winter. This result indicates that the chemical process or transport, rather than the precursor, plays a critical role in controlling the variations in iSOA concentrations. However, the 2-MG and 2-MG-OS were biased low (Figure 3d and 3e), which is in consistent with previous simulations at 14 sites across China in summer (Qin et al., 2018). The larger uncertainties of simulated HMML/MAE-SOA tracers might be attributed to the lack of well constrained kinetic parameters for reactive uptake of HMML/MAE. In addition, simulated concentrations of iSOA tracer species had decreasing inter-annual trend in both Base Case and Case 1 (Figure S3), which was in agreement with observations of total iSOA and IEPOX-SOA, but not for HMML/MAE-SOA species. This result suggests that the major factors driving the overall formation and evolution of iSOA and in particular IEPOX-SOA were captured by the model, while some factors governing the abundance of HMML/MAE-SOA might not be well represented in the model.

https://doi.org/10.5194/egusphere-2025-1909
Preprint. Discussion started: 15 May 2025


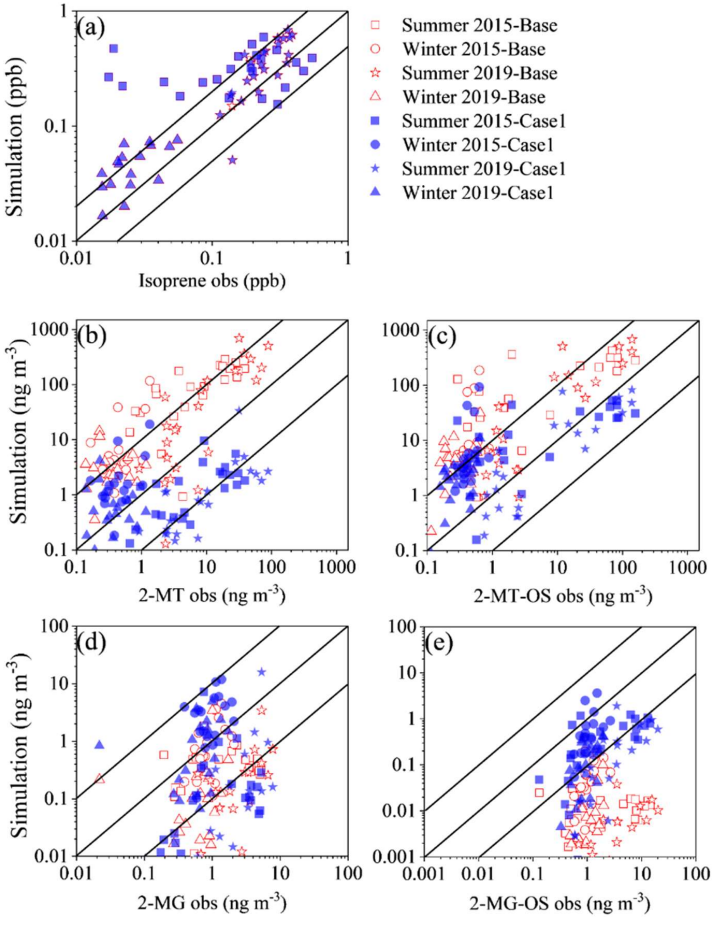


Figure 3. Comparisons of simulations against observations for (a) isoprene, (b) 2-MTs, (c) 2-MT-OS, (d) 2-MG, (e) 2-MG-OS in summer and winter of 2015 and 2019. Red dot represents simulations with standard CMAQ v5.2 (Base Case), and blue represents simulations using the optimized model (Case 1). The 1:1, 10:1, and 1:10 lines are shown with solid lines.

The gas-phase and particle-phase fractions of 2-MG and 2-MTs were estimated using a chemical equilibrium partitioning model as described in Section S3 and the results are shown in Figure S4. The particle-phase fraction ($F_p$) of 2-MG was highly variable, with a significant lower value in summer (9.0 -19.0%) than in winter (31.6 - 44.0%), indicating substantial amounts of 2-MG was present in the gas phase in summer. Additionally, the $F_p$ value of iSOA polyols, in particular for 2-MG, decreased yearly. As a result, the gas-plus-particle-phase concentrations of 2-MG showed an upward trend in summer

https://doi.org/10.5194/egusphere-2025-1909
Preprint. Discussion started: 15 May 2025


from 2015-2021 ($p < 0.05$, Figure S4). In contrast, 2-MTs were mainly distributed in the particle phase with $F_p$ values larger than 70% in both seasons, consistent with previous measurements (Isaacman-Vanwertz et al., 2016). The inter-annual trend of 2-MT was not significantly affected by their gas-phase fraction because of the relatively low volatility. Overall, the total HMML/MAE-SOA exhibited a distinctly different inter-annual trend compared to IEPOX-SOA in summer over 2015-2021. It should be noted that although the measured concentrations of iSOA tracers could be affected by quantification uncertainties including matrix effect and the use of surrogate standards, their inter-annual trends were not affected by these uncertainties. The key factors driving such trends will be discussed in detail in Sections 3.2 and 3.3.

As shown in Table S1, the concentration ratios of IEPOX-SOA to HMML/MAE-SOA in the particle phase decreased in both summer (11.1 ± 6.7, 7.8 ± 6.3, and 5.6 ± 3.0 in 2015, 2019, and 2021, respectively) and winter (0.8 ± 0.3, 0.8 ± 0.2, and 0.7 ± 0.4). This result indicates an increasing contribution of $NO_x$-influenced pathways to iSOA formation despite the strong anthropogenic emission reductions from 2015 to 2021 in Shanghai. Accounting for the gas-particle partitioning of 2-MTs and 2-MG as well as the quantification uncertainties for iSOA tracers do not significantly change such a decreasing trend. However, it significantly decreases the ratio values of IEPOX-SOA to HMML/MAE-SOA to 2.63 ± 1.93, 1.55 ± 2.15, and 0.90 ± 0.81 in summer and 0.39 ± 0.15, 0.33 ± 0.11, and 0.29 ± 0.17 in winter of 2015, 2019, and 2021, respectively, suggesting that the corrected gas-plus-particle-phase concentration of HMML/MAE-SOA tracers was comparable to that of IEPOX-SOA tracers. This result emphasizes the importance of considering the gas-particle partitioning of polyols for a deeper understanding of the abundance and formation characteristics of iSOA.

### 3.3 Key influencing factors of iSOA formation

The production of iSOA can be influenced by a variety of factors such as the emission and concentration of isoprene, atmospheric oxidizing capacity as represented by the concentrations of $O_3$ or odd oxygen ($O_x = O_3 + NO_2$), nitrogen oxides, as well as aerosol composition and properties including sulfate content, acidity, and LWC. Here, we identify the major influencing factors of IEPOX-SOA and HMML/MAE-SOA formation through the correlation analysis between different iSOA tracers and influencing factors (Figure 4).

https://doi.org/10.5194/egusphere-2025-1909
Preprint. Discussion started: 15 May 2025


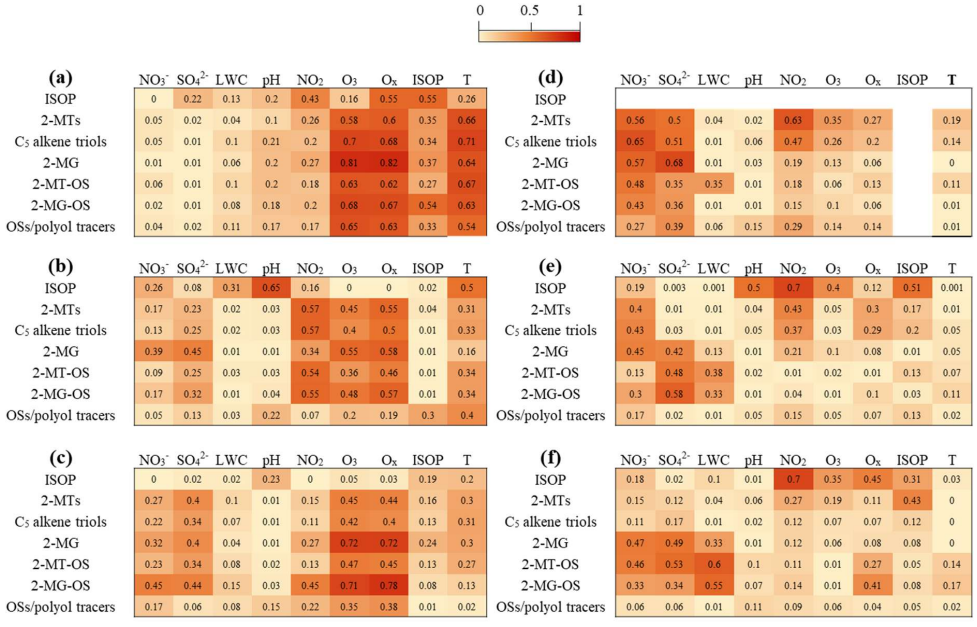


Figure 4. Coefficients of correlation ($r^2$) between iSOA compounds and various influencing factors of iSOA formation in (a-c) summer and (d-f) winter of 2015, 2019, and 2021, respectively.

The correlations of all iSOA species with isoprene were relatively weak, with most of the correlation coefficients ($r^2$) below 0.37. Therefore, the decline in iSOA concentrations from 2015 to 2021 could not be attributed to the slight variation in isoprene concentration. The HMML/MAE-SOA species exhibited strong correlations with ozone ($r^2$ = 0.48-0.81) and $O_x$ ($r^2$ = 0.57-0.82) in summer, in particular in 2015 and 2021 while exhibiting relatively weaker correlations with $NO_2$ ($r^2$ = 0.20-0.55). Such correlations between 2-MG and ozone were also observed in previous measurements in southeastern US (Rattanavaraha et al., 2016), which proposed that ozone might be a superior indicator to $NO_x$ for the photochemical process of isoprene under $NO_x$-dominant conditions. The IEPOX-SOA tracers also correlated well with ozone ($r^2$ = 0.36-0.70) or $O_x$ ($r^2$ = 0.40-0.68) in summer, despite less strongly than HMML/MAE-SOA species. These observations clearly suggest that atmospheric oxidation capacity (or the oxidation of isoprene to epoxide intermediates) plays a driving role in summertime iSOA formation. In addition, moderate correlations ($r^2$ = 0.23-0.45) were observed between the iSOA tracers and sulfate aerosol in 2019 and 2021, indicating that sulfate aerosol also plays a role in controlling iSOA formation during these periods. In contrast, wintertime iSOA species

https://doi.org/10.5194/egusphere-2025-1909
Preprint. Discussion started: 15 May 2025


exhibited weak correlations with $O_3$ and $O_x$ in all the three years (Figure 4d-f). However, they all had moderate or strong correlations with sulfate aerosol ($r^2$ = 0.36-0.68) in 2015 and the iSOA OSs correlated well with sulfate ($r^2$ = 0.35-0.58) and LWC ($r^2$ = 0.34-0.58) in 2019 and 2021. These results suggest that sulfate-mediated heterogeneous chemistry of isoprene epoxide intermediates in aqueous aerosols is a key process controlling iSOA formation in winter (Surratt et al., 2010; Lin et al., 2012; Yee et al., 2020).

As shown in Table S1, the concentrations of sulfate aerosol and LWC both decreased drastically over 2015-2021, which could explain the declining trend of iSOA in winter and partially contributed to the decreased formation of IEPOX-SOA in summer. Notably, the summertime average MDA8 (maximum daily 8-h average) $O_3$ concentration at the observation site increased from 2015 to 2017 and then decreased significantly in 2018, followed by a slight increasing trend between 2018 and 2021 (Figure S5). This inter-annual trend of $O_3$ was similar to the trend of annual 90$^{th}$ percentile MDA8 $O_3$ concentration in the region of Shanghai (Figure S5). As a result, the summertime average MDA8 $O_3$ concentration in 2015, 2019, and 2021 showed a slight downward trend. In addition, the simulated concentrations of OH radicals and ratios of (MVK+MACR)/isoprene both declined in 2019 compared to those in 2015 (see Table S5), indicating a decline in the atmospheric oxidation capacity during the observation period. Similarly, the nighttime atmospheric oxidation capacity as indicated by the production rate of $NO_3$ radicals ($PNO_3$), calculated by multiplying the reaction rate coefficient between $NO_2$ and $O_3$ by their concentrations (Wang et al., 2023a), also decreased during this period (Figure S6). The reduced atmospheric oxidation capacity further explained the decreased formation of IEPOX-SOA in summer during these years, but it could not explain the inter-annual variation in summertime HMML/MAE-SOA, suggesting that other factors might have offset the anticipated decline in HMML/MAE-SOA during this period.

### 3.4 Heterogeneous reactivity of ambient aerosols

To better understand the role of heterogeneous chemistry in the formation and inter-annual variations of iSOA, the reactive uptake coefficients ($\gamma_{EPOXIDE}$) of isoprene-derived epoxides on ambient aerosols were estimated by a resistor model (eq. 4) (Xu et al., 2016; Pye et al., 2013). The pseudo-first-order heterogeneous reaction rate constant ($k_{het}$, $s^{-1}$) of gas-phase IEPOX and HMML/MAE could be

https://doi.org/10.5194/egusphere-2025-1909
Preprint. Discussion started: 15 May 2025


then estimated from $\gamma_{EPOXIDE}$ via eq. 7. Currently, there are four sets of reported third-order reaction rate constants (i.e., $k_{i,j}$ in eq. 1) for the acid-catalyzed nucleophilic addition of water and sulfate to IEPOX in the aqueous phase (Table 1). Piletic et al. (2013) predicted $k_{i,j}$ for IEPOX ($k_{i,j\text{-}IEPOX}^{-1}$) with a computational model, which are two orders of magnitudes higher than the laboratory-measured values ($k_{i,j\text{-}IEPOX}^{-2}$) by Riedel et al. (2015) and model-estimated values ($k_{i,j\text{-}IEPOX}^{-3}$) using CMAQ by Pye et al. (2013). More recently, Pye et al. (2017) updated the values ($k_{i,j\text{-}IEPOX}^{-4}$) by constraining the $k_{i,j\text{-}IEPOX}^{-3}$ using measured 2-MT-OS/2-MTs in CMAQ. For HMML/MAE, there is a lack of direct measurements and theoretical calculations of their $k_{i,j}$ values. Pye et al. (2013) assumed the same $k_{i,j}$ values as IEPOX with $k_{i,H^+}$ of $9.0 \times 10^{-4}$ $M^{-2}$ $s^{-1}$ for water and $2.0 \times 10^{-4}$ $M^{-2}$ $s^{-1}$ for sulfate.

Table 1. Third-order reaction rate constants of IEPOX and HMML/MAE with sulfate and water in the aqueous phase

| | $k_{i,H^+}$ ($M^{-2}\cdot s^{-1}$) | | $k_{i,HSO_4^-}$ ($M^{-2}\cdot s^{-1}$) | | References |
|---|---|---|---|---|---|
| | $i=H_2O$ | $i=SO_4^{2-}$ | $i=H_2O$ | $i=SO_4^{2-}$ | |
| $k_{i,j\text{-}IEPOX}^{-1}$ | $5.3\times10^{-2}$ | $5.2\times10^{-1}$ | — | — | (Piletic et al., 2013) |
| $k_{i,j\text{-}IEPOX}^{-2}$ | $3.4\times10^{-4}$ | $4.8\times10^{-4}$ | — | — | (Riedel et al., 2015) |
| $k_{i,j\text{-}IEPOX}^{-3}$ | $9\times10^{-4}$ | $2\times10^{-4}$ | $1.3\times10^{-5}$ | $2.9\times10^{-6}$ | (Pye et al., 2013) |
| $k_{i,j\text{-}IEPOX}^{-4}$ | $9\times10^{-4}$ | $8.8\times10^{-3}$ | $1.3\times10^{-5}$ | $2.9\times10^{-6}$ | (Pye et al., 2017) |
| $k_{i,j\text{-}HMML/MAE}$ | $9\times10^{-4}$ | $2\times10^{-4}$ | $1.3\times10^{-5}$ | $2.9\times10^{-6}$ | (Pye et al., 2013) |
| $k_{i,j\text{-}HMML/MAE}^{-1}$ | $9\times10^{-4}$ | $2\times10^{-3}$ | $1.3\times10^{-5}$ | $2.9\times10^{-6}$ | — |
| $k_{i,j\text{-}HMML/MAE}^{-2}$ | $9\times10^{-4}$ | $2\times10^{-2}$ | $1.3\times10^{-5}$ | $2.9\times10^{-6}$ | — |

Firstly, the $k_{i,j}$ values of IEPOX and HMML/MAE were evaluated by comparing the measured ratios of 2-MT-OS/2-MTs and 2-MG-OS/2-MG with the calculated ratios of the pseudo-first-order rate constants for the nucleophilic addition reactions of epoxides with sulfate and water ($k_{aq,\ SO_4^{2-}}/k_{aq,\ H_2O}$). The results are shown in Figure S7 and S8 For IEPOX, the $k_{aq,\ SO_4^{2-}}/k_{aq,\ H_2O}$ ratios were close to measured particulate ratios of 2-MT-OS/2-MTs when using $k_{i,j\text{-}IEPOX}^{-1}$ and $k_{i,j\text{-}IEPOX}^{-4}$ suggested by Piletic et al. (2013) and Pye et al. (2017), respectively. That was still the case when taking into account the quantification uncertainties and the gas-phase fractions of 2-MT-OS and 2-MTs. However, the calculated $k_{aq,\ SO_4^{2-}}/k_{aq,\ H_2O}$ ratios for HMML/MAE were 1-2 orders of magnitude lower than the

https://doi.org/10.5194/egusphere-2025-1909
Preprint. Discussion started: 15 May 2025


measured 2-MG-OS/2-MG ratios (Figure S7). This result indicates that the $k_{ij}$ of HMML/MAE with sulfate was likely underestimated, since Pye et al. (2013) found the hydrolysis rate constant of HMML/MAE could lead to a good prediction of the concentration of 2-MG. Therefore, the $k_{i,j}$ of HMML/MAE with sulfate was elevated by one ($k_{i,j\text{-HMML}}^{-1}$) to two ($k_{i,j\text{-HMML}}^{-2}$) orders of magnitude to estimate the $k_{het}$ of HMML/MAE.

Figure 5 shows the γ and $k_{het}$ values for IEPOX and HMML/MAE estimated using different sets of kinetic parameters listed in Table 1. The CMAQ-modeled values are also displayed for comparison. The value of $k_{het}$ for HMML/MAE calculated by elevated $k_{i,j\text{-HMML}}^{-1}$ and $k_{i,j\text{-HMML}}^{-2}$ increased by about one and two folds (shown in Figure 5c), respectively. However, the inter-annual trend of $k_{het\text{-HMML}}$ was unaltered. In addition, the $k_{het}$ estimated by $k_{i,j\text{-IEPOX}}^{-1}$ and $k_{i,j\text{-IEPOX}}^{-2}$ in summer had highest values in 2019. This might be attributed to the fact that these two sets of parameters lack the third-order reaction rate constant of IEPOX with nucleophiles catalyzed by bisulfate (Table 1). As a comparison, we calculated the $k_{het}$ of IEPOX and HMML/MAE excluding the reaction rate constant catalyzed by bisulfate (Figure S9). We found that the inter-annual trend of IEPOX (Figure S9a) and HMML/MAE (Figure S9b) in summertime was altered and similar to that of IEPOX calculated by $k_{i,j\text{-IEPOX}}^{-1}$ and $k_{i,j\text{-IEPOX}}^{-2}$. While the inter-annual trend of $k_{het}$ in winter was not sensitive to the exclusion of reaction rate constant catalyzed by bisulfate. This result indicates a contribution of nucleophilic-addition of epoxides catalyzed by bisulfate to the heterogeneous reactivity. It is also proved that the $k_{i,j\text{-IEPOX}}^{-4}$ is more appreciate for predicting the measured ratios of 2-MT-OS to 2-MTs and the aerosol heterogeneous reactivity toward IEPOX.

As shown in Figure 5a and 5c, the estimated γ and $k_{het}$ of IEPOX and HMML/MAE using $k_{i,j\text{-IEPOX}}^{-4}$, $k_{i,j\text{-HMML}}^{-1}$, and $k_{i,j\text{-HMML}}^{-2}$ showed a similar trend which decreased in both winter and summer. Similar decreasing trends in γ and $k_{het}$ were also simulated by CMAQ (Figure 5b and 5d). The calculated γ and $k_{het}$ values of IEPOX and HMML/MAE in summer using $k_{i,j\text{-IEPOX}}^{-4}$ and $k_{i,j\text{-HMML}}$, respectively, are consistent with the simulated results, while the calculated values in winter were significantly lower than the simulations, which is likely attributed to the significantly under-predicted aerosol pH and thereby over-predicted aerosol reactivity in winter by the model. Overall, the declining trend of both calculated

https://doi.org/10.5194/egusphere-2025-1909
Preprint. Discussion started: 15 May 2025


and model-predicted $k_{het}$ offers an explanation for the decreasing trend of iSOA in both seasons and IEPOX-SOA in summer, but it could not explain the observed trend of HMML/MAE-SOA in summer.

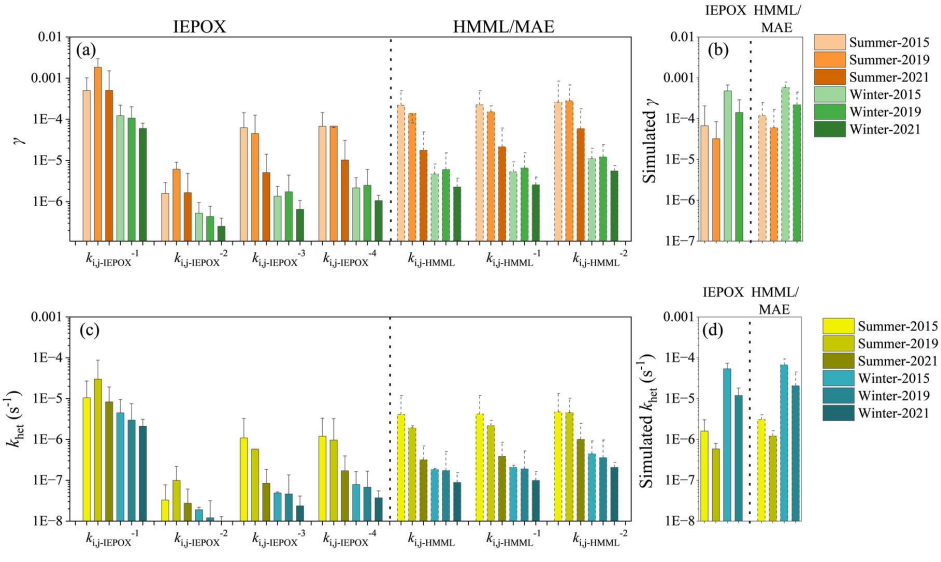


Figure 5. Reactive uptake coefficients (γ) and pseudo-first-order heterogeneous reaction rate constant ($k_{het}$, s$^{-1}$) of gas-phase IEPOX and HMML/MAE estimated using different sets of $k_{i,j\text{-IEPOX}}$ and $k_{i,j\text{-HMML}}$ listed in Table 1 (a and c) and simulated by CMAQ model in Case 1 (b and d).

### 3.5 Meteorological influences on iSOA variation

As discussed above, the variations in chemical factors (including atmospheric oxidizing capacity and aerosol heterogeneous reactivity) could well explain the declining trend of both summertime and wintertime IEPOX-SOA and wintertime HMML/MAE-SOA, but not the trend of summertime HMML/MAE-SOA during the period of 2015-2021. Since meteorological conditions could exert a significant influence on the concentrations of atmospheric pollutants (Liu et al., 2023b; Gu et al., 2023), we further investigate the impact of the variation in meteorological conditions on the variation of iSOA during the observation period.

To do so, the CMAQ simulations for 2019 adopted the emissions of 2015 (Test Case), so the variations in simulated iSOA concentration from 2015 to 2019 in this case is mainly attributed to the changes in the meteorological conditions during these years. As shown in Figure 6, the simulated concentrations of 2-MTs, 2-MT-OS, 2-MG, and 2-MG-OS in 2019 decreased by 45.7%, 85.9%, 57.0%,

https://doi.org/10.5194/egusphere-2025-1909
Preprint. Discussion started: 15 May 2025


and 70.9% in summer and 61.2 %, 38.4%, 53.2%, and 75.6% in winter, respectively, compared to the concentrations in 2015 in the Test Case. Such decreases were close to the concentration reductions simulated in the Case 1, suggesting that the alteration in meteorological conditions exerts a more substantial influence on the variation in iSOA concentrations compared to the changes in emissions.

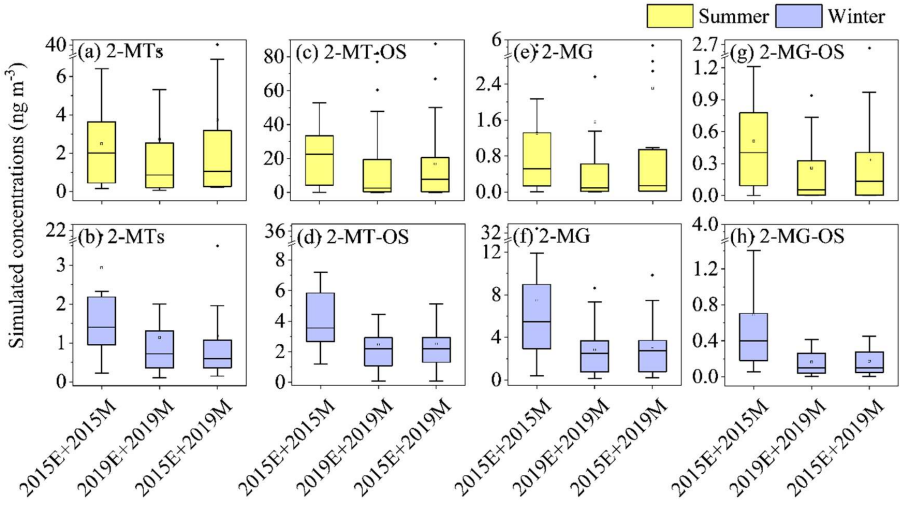


Figure 6. Simulated concentrations of 2-MTs, 2-MT-OS, 2-MG and 2-MG-OS in summer (a, c, e and g) and winter (b, d, f and h) in Case 1 (2015E+2015M vs. 2019E+2019M) and Test Case (2015E+2015M vs. 2015E+2019M).

It should be noted that the variations in meteorological conditions not only affect the physical processes such as dilution and transport, but also influence the chemical processes determining the formation of iSOA. To investigate the impacts of physical and chemical factors associated with the variations in meteorological conditions on the abundance of iSOA, the concentrations of elemental carbon (EC) were simulated in the Test Case. As shown in Figure 7, the simulated average concentrations of summertime and wintertime EC in 2019 decreased by 15.9% and 22.1%, respectively, compared to those in 2015. Since EC is a primary pollutant and chemically inert under atmospheric conditions, the variations in its concentration in the Test Case is attributed to the changes in the physical processes. As a result, we could expect a similar contribution of the physical processes to the reduction in iSOA concentration (15.9% in summer and 22.1% in winter). Notably, such reductions are significantly smaller than the simulated concentration reductions of iSOA in the Test case (Figure 6),

https://doi.org/10.5194/egusphere-2025-1909
Preprint. Discussion started: 15 May 2025


suggesting that the chemical factors associated with the changes in meteorological conditions play a crucial role in determining the trend of iSOA in Shanghai, consistent with the above analysis based on the observations. However, we note that the alternation in meteorological conditions cannot explain the observed non-declining trend of HMML/MAE-SOA in summer, implying that some other factors that are not well represented in the CMAQ model may play a role in controlling such a trend.

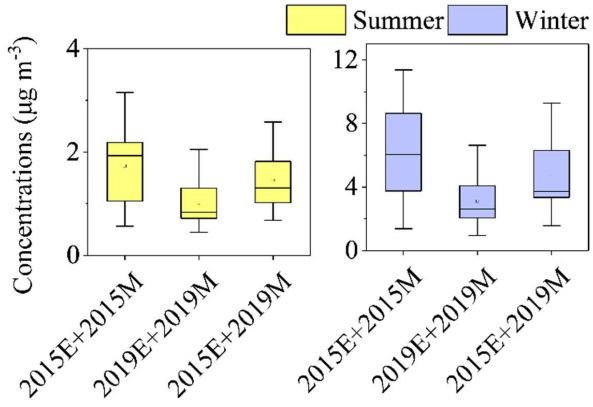


Figure 7. Simulated EC concentrations in Case 1 (2015E+2015M vs. 2019E+2019M) and Test Case (2015E+2015M vs. 2015E+2019M).

As the precursor to HMML and MAE, the MACR can be derived from both primary sources, such as biological emissions (Jardine et al., 2012), residential wood burning (Gaeggeler et al., 2008), vehicle exhaust emissions (He et al., 2009), and secondary formation from gas-phase oxidation of isoprene (Schwantes et al., 2015; Surratt et al., 2010). Field studies have demonstrated that the concentration of MACR in urban areas was predominantly influenced by vehicle emissions (Park et al., 2011; Ling et al., 2019). In the present work, the simulated MACR concentration demonstrated a decreasing trend from 2015 to 2019 in summer when the contribution of primary emissions was considered in the model. Yet, our recent study revealed that, despite a good agreement between modelled and measured isoprene concentrations, the model under-predicted the peak concentrations of MACR during the noon in urban Shanghai (Li et al., 2022), implying an underestimation of secondary formation and/or primary emissions of MACR in the model. Furthermore, Gu et al. (2023) reported that in the southern cities of Jiangsu Province, which is adjacent to Shanghai, anthropogenic VOCs increased by approximately 15% from 2015 to 2019. Therefore, we infer that the sources (e.g., primary emissions) of MACR might be

https://doi.org/10.5194/egusphere-2025-1909
Preprint. Discussion started: 15 May 2025


underappreciated in this work, which may provide a rationale for the under-prediction of HMML/MAE-SOA concentrations and the inconsistency between its simulated and observed inter-annual trends.

## 4. Conclusions

In this study, three-year-measurements of isoprene-derived SOA species in ambient $PM_{2.5}$ were conducted at an urban site in Shanghai, China during the period of 2015-2021, aiming to understand the response of biogenic SOA formation to anthropogenic emission reductions in polluted regions. The complementary CMAQ model simulations were also performed for 2015 and 2019 and the results are compared to the measurements. It is found that the particulate concentration of total iSOA tracers had a decreasing trend from 2015 to 2021 (55.6, 51.0, and 29.7 ng $m^{-3}$ in 2015, 2019, and 2021, respectively), with a dominant contribution from IEPOX-SOA species (52.6, 46.7, and 25.8 ng $m^{-3}$ in 2015, 2019, and 2021, respectively), while HMML/MAE-SOA species (4.3, 4.2, and 4.3 ng $m^{-3}$ in 2015, 2019, and 2021, respectively) did not decrease significantly and, after accounting for their gas-phase fraction, even exhibited a slight upward trend in summer during these years. The different inter-annual trend of 2-MTs, as compared to other IEPOX-SOA species such as $C_5$-alkene triols and 2-MT-OS, is likely ascribed to the contributions of non-secondary sources (e.g., direct biological emissions) to this type of species.

The isoprene-derived SOA species correlated well with ozone and $O_x$ in summer but with sulfate in winter, suggesting that the atmospheric oxidation of isoprene to epoxide intermediates and their subsequent reactive uptake on aqueous aerosols are the key steps driving the formation of iSOA in summer and winter, respectively. The $O_3$ and Ox-represented atmospheric oxidizing capacity as well as the kinetically estimated aerosol heterogeneous reactivity decreased significantly during the observation period, which provided an explanation for the decreasing trend of IEPOX-SOA and wintertime HMML/MAE-SOA, but not the summertime HMML/MAE-SOA.

The CMAQ model predicted the levels of iSOA tracers reasonably well and captured the declining trend of measured IEPOX-SOA in both seasons and HMML/MAE-SOA in winter. However, the predicted declining trend of HMML/MAE-SOA in summer was contrary to the observed trend. Further model simulations show that inter-annual variations in iSOA concentration are mainly governed by the changes in the meteorological conditions rather than the emissions. Consistent with the analysis based on the observation data, the model simulations show that the changes in chemical factors such as aerosol

https://doi.org/10.5194/egusphere-2025-1909
Preprint. Discussion started: 15 May 2025


heterogeneous reactivity caused by variations in meteorological conditions play an important role in controlling the inter-annual trend of iSOA. The model results also suggest the presence of unaccounted or underrepresented factors such as the direct emissions of MACR in the model, which led to the discrepancy between the modeled and observed trends of HMML/MAE-SOA in summer. Overall, our study revealed the responses and underlying driving factors of iSOA formation under rapidly changing anthropogenic emissions conditions in typical Chinese megacities. It also highlights the importance of regulating chemical factors such as atmospheric oxidizing capacity and aerosol chemical reactivity in the mitigation of the PM pollution from biogenic emissions.

**Data availability.**

The data presented in this work are available upon request from the corresponding author.

**Competing interests.**

The authors declare no competing interest relevant to this study.

**Author Contributions.**

YZ conceived and designed the study, HH, YW, and TY performed the field observation and analyzed the data, JL, YL, TL, and YS performed the model simulations, HH, YZ, and JL wrote the paper, and all other authors contributed to the discussion and writing.

**Acknowledgements.**

This study was supported by the National Key R&D Program of China (no. 2022YFC3701003) and the National Natural Science Foundation of China (no. 22376137 and 22206120).

**References**

Bates, K. H., Crounse, J. D., St. Clair, J. M., Bennett, N. B., Nguyen, T. B., Seinfeld, J. H., Stoltz, B. M., and Wennberg, P. O.: Gas Phase Production and Loss of Isoprene Epoxydiols, J. Phys. Chem. A, 118, 1237-1246, 10.1021/jp4107958, 2014.

Bryant, D. J., Elzein, A., Newland, M., White, E., Swift, S., Watkins, A., Deng, W., Song, W., Wang, S., Zhang, Y., Wang, X., Rickard, A. R., and Hamilton, J. F.: Importance of Oxidants and Temperature in the Formation of Biogenic Organosulfates and Nitrooxy Organosulfates, ACS Earth Space Chem, 5, 2291-2306, 10.1021/acsearthspacechem.1c00204, 2021.

https://doi.org/10.5194/egusphere-2025-1909
Preprint. Discussion started: 15 May 2025


Budisulistiorini, S. H., Li, X., Bairai, S. T., Renfro, J., Liu, Y., Liu, Y. J., McKinney, K. A., Martin, S. T., McNeill, V. F., Pye, H. O. T., Nenes, A., Neff, M. E., Stone, E. A., Mueller, S., Knote, C., Shaw, S. L., Zhang, Z., Gold, A., and Surratt, J. D.: Examining the effects of anthropogenic emissions on isoprene-derived secondary organic aerosol formation during the 2013 Southern Oxidant and Aerosol Study (SOAS) at the Look Rock, Tennessee ground site, Atmos. Chem. Phys., 15, 8871-8888, 10.5194/acp-15-8871-2015, 2015.

Ding, X., He, Q. F., Shen, R. Q., Yu, Q. Q., and Wang, X. M.: Spatial distributions of secondary organic aerosols from isoprene, monoterpenes, beta-caryophyllene, and aromatics over China during summer, J Geophys Res-atmos, 119, 11877-11891, Doi 10.1002/2014jd021748, 2014.

Eddingsaas, N. C., VanderVelde, D. G., and Wennberg, P. O.: Kinetics and Products of the Acid-Catalyzed Ring-Opening of Atmospherically Relevant Butyl Epoxy Alcohols, J. Phys. Chem. A, 114, 8106-8113, 10.1021/jp103907c, 2010.

Fan, Y., Liu, C.-Q., Li, L., Ren, L., Ren, H., Zhang, Z., Li, Q., Wang, S., Hu, W., Deng, J., Wu, L., Zhong, S., Zhao, Y., Pavuluri, C. M., Li, X., Pan, X., Sun, Y., Wang, Z., Kawamura, K., Shi, Z., and Fu, P.: Large contributions of biogenic and anthropogenic sources to fine organic aerosols in Tianjin, North China, Atmos. Chem. Phys., 20, 117-137, 10.5194/acp-20-117-2020, 2020.

Frauenheim, M., Offenberg, J., Zhang, Z., Surratt, J. D., and Gold, A.: The $C_5$–Alkene Triol Conundrum: Structural Characterization and Quantitation of Isoprene-Derived $C_5H_{10}O_3$ Reactive Uptake Products, Environ. Sci. Technol. Lett., 9, 829-836, 10.1021/acs.estlett.2c00548, 2022.

Fu, P., Aggarwal, S. G., Chen, J., Li, J., Sun, Y., Wang, Z., Chen, H., Liao, H., Ding, A., Umarji, G. S., Patil, R. S., Chen, Q., and Kawamura, K.: Molecular Markers of Secondary Organic Aerosol in Mumbai, India, Environ Sci Technol, 50, 4659-4667, 10.1021/acs.est.6b00372, 2016.

Fu, P. Q., Kawamura, K., Chen, J., and Miyazaki, Y.: Secondary Production of Organic Aerosols from Biogenic VOCs over Mt. Fuji, Japan, Environ Sci Technol, 48, 8491-8497, 10.1021/es500794d, 2014.

Fu, P. Q., Kawamura, K., Chen, J., Li, J., Sun, Y. L., Liu, Y., Tachibana, E., Aggarwal, S. G., Okuzawa, K., Tanimoto, H., Kanaya, Y., and Wang, Z. F.: Diurnal variations of organic molecular tracers and stable carbon isotopic composition in atmospheric aerosols over Mt. Tai in the North China Plain: an influence of biomass burning, Atmos. Chem. Phys., 12, 8359-8375, 10.5194/acp-12-8359-2012, 2012.

Gaeggeler, K., Prevot, A. S. H., Dommen, J., Legreid, G., Reimann, S., and Baltensperger, U.: Residential wood burning in an Alpine valley as a source for oxygenated volatile organic compounds, hydrocarbons and organic acids, Atmos. Environ, 42, 8278-8287, 10.1016/j.atmosenv.2008.07.038, 2008.

Geng, G., Liu, Y., Liu, Y., Liu, S., Cheng, J., Yan, L., Wu, N., Hu, H., Tong, D., Zheng, B., Yin, Z., He, K., and Zhang, Q.: Efficacy of China's clean air actions to tackle $PM_{2.5}$ pollution between 2013 and 2020, Nat. Geosci, 17, 987-994, 10.1038/s41561-024-01540-z, 2024.

Gong, J., Yin, Z., Lei, Y., Lu, X., Zhang, Q., Cai, C., Chai, Q., Chen, H., Chen, R., Chen, W., Cheng, J., Chi, X., Dai, H., Dong, Z., Geng, G., Hu, J., Hu, S., Huang, C., Li, T., Li, W., Li, X., Lin, Y., Liu, J., Ma, J., Qin, Y., Tang, W., Tong, D., Wang, J., Wang, L., Wang, Q., Wang, X., Wang, X., Wu, L., Wu, R., Xiao, Q., Xie, Y., Xu, X., Xue, T., Yu, H., Zhang, D., Zhang, L., Zhang, N., Zhang, S., Zhang, S., Zhang, X., Zhang, Z., Zhao, H., Zheng, B., Zheng, Y., Zhu, T., Wang, H., Wang, J., and He, K.: The 2023 report of the synergetic roadmap on carbon neutrality and clean air for China: Carbon reduction, pollution mitigation,

https://doi.org/10.5194/egusphere-2025-1909
Preprint. Discussion started: 15 May 2025


greening, and growth, Environ. Sci. Ecotechnol., 23, 100517, https://doi.org/10.1016/j.ese.2024.100517, 2025.

Gu, C., Zhang, L., Xu, Z., Xia, S., Wang, Y., Li, L., Wang, Z., Zhao, Q., Wang, H., and Zhao, Y.: High-resolution regional emission inventory contributes to the evaluation of policy effectiveness: a case study in Jiangsu Province, China, Atmos. Chem. Phys., 23, 4247-4269, 10.5194/acp-23-4247-2023, 2023.

Guenther, A., Karl, T., Harley, P., Wiedinmyer, C., Palmer, P. I., and Geron, C.: Estimates of global terrestrial isoprene emissions using MEGAN (Model of Emissions of Gases and Aerosols from Nature), Atmos. Chem. Phys., 6, 3181-3210, 10.5194/acp-6-3181-2006, 2006.

He, C., Ge, Y. S., Tan, J. W., You, K. W., Han, X. K., Wang, J. F., You, Q. W., and Shah, A. N.: Comparison of carbonyl compounds emissions from diesel engine fueled with biodiesel and diesel, Atmos. Environ, 43, 3657-3661, 10.1016/j.atmosenv.2009.04.007, 2009.

He, Q.-F., Ding, X., Fu, X.-X., Zhang, Y.-Q., Wang, J.-Q., Liu, Y.-X., Tang, M.-J., Wang, X.-M., and Rudich, Y.: Secondary Organic Aerosol Formation From Isoprene Epoxides in the Pearl River Delta, South China: IEPOX- and HMML-Derived Tracers, J Geophys Res-atmos, 123, 6999-7012, 10.1029/2017jd028242, 2018.

He, Q.-F., Ding, X., Wang, X.-M., Yu, J.-Z., Fu, X.-X., Liu, T.-Y., Zhang, Z., Xue, J., Chen, D.-H., Zhong, L.-J., and Donahue, N. M.: Organosulfates from Pinene and Isoprene over the Pearl River Delta, South China: Seasonal Variation and Implication in Formation Mechanisms, Environ Sci Technol, 48, 9236-9245, 10.1021/es501299v, 2014.

Heald, C. L., Henze, D. K., Horowitz, L. W., Feddema, J., Lamarque, J. F., Guenther, A., Hess, P. G., Vitt, F., Seinfeld, J. H., Goldstein, A. H., and Fung, I.: Predicted change in global secondary organic aerosol concentrations in response to future climate, emissions, and land use change, J Geophys Res-atmos, 113, 10.1029/2007jd009092, 2008.

Hennigan, C. J., Izumi, J., Sullivan, A. P., Weber, R. J., and Nenes, A.: A critical evaluation of proxy methods used to estimate the acidity of atmospheric particles, Atmos. Chem. Phys., 15, 2775-2790, 10.5194/acp-15-2775-2015, 2015.

Hettiyadura, A. P. S., Stone, E. A., Kundu, S., Baker, Z., Geddes, E., Richards, K., and Humphry, T.: Determination of atmospheric organosulfates using HILIC chromatography with MS detection, Atmos. Meas. Tech., 8, 2347-2358, 10.5194/amt-8-2347-2015, 2015.

Hu, D., Bian, Q., Li, T. W. Y., Lau, A. K. H., and Yu, J. Z.: Contributions of isoprene, monoterpenes, β-caryophyllene, and toluene to secondary organic aerosols in Hong Kong during the summer of 2006, J Geophys Res-atmos, 113, https://doi.org/10.1029/2008JD010437, 2008.

Huang, R.-J., Zhang, Y., Bozzetti, C., Ho, K.-F., Cao, J.-J., Han, Y., Daellenbach, K. R., Slowik, J. G., Platt, S. M., Canonaco, F., Zotter, P., Wolf, R., Pieber, S. M., Bruns, E. A., Crippa, M., Ciarelli, G., Piazzalunga, A., Schwikowski, M., Abbaszade, G., Schnelle-Kreis, J., Zimmermann, R., An, Z., Szidat, S., Baltensperger, U., Haddad, I. E., and Prévôt, A. S. H.: High secondary aerosol contribution to particulate pollution during haze events in China, Nature, 514, 218-222, 10.1038/nature13774, 2014.

Isaacman-VanWertz, G., Yee, L. D., Kreisberg, N. M., Wernis, R., Moss, J. A., Hering, S. V., de Sá, S. S., Martin, S. T., Alexander, M. L., Palm, B. B., Hu, W., Campuzano-Jost, P., Day, D. A., Jimenez, J. L., Riva, M., Surratt, J. D., Viegas, J., Manzi, A., Edgerton, E., Baumann, K., Souza, R., Artaxo, P., and Goldstein,

https://doi.org/10.5194/egusphere-2025-1909
Preprint. Discussion started: 15 May 2025


A. H.: Ambient Gas-Particle Partitioning of Tracers for Biogenic Oxidation, Environ Sci Technol, 50, 9952-9962, 10.1021/acs.est.6b01674, 2016.

Jardine, K. J., Monson, R. K., Abrell, L., Saleska, S. R., Arneth, A., Jardine, A., Ishida, F. Y., Serrano, A. M. Y., Artaxo, P., Karl, T., Fares, S., Goldstein, A., Loreto, F., and Huxman, T.: Within-plant isoprene oxidation confirmed by direct emissions of oxidation products methyl vinyl ketone and methacrolein, Global Change Biol. , 18, 973-984, 10.1111/j.1365-2486.2011.02610.x, 2012.

Kang, M. J., Fu, P. Q., Kawamura, K., Yang, F., Zhang, H. L., Zang, Z. C., Ren, H., Ren, L. J., Zhao, Y., Sun, Y. L., and Wang, Z. F.: Characterization of biogenic primary and secondary organic aerosols in the marine atmosphere over the East China Sea, Atmos. Chem. Phys., 18, 13947-13967, 10.5194/acp-18-13947-2018, 2018.

Kebarle, P.: A brief overview of the present status of the mechanisms involved in electrospray mass spectrometry, J Mass Spectrom, 35, 804-817, 10.1002/1096-9888(200007)35:7<804::Aid-jms22>3.0.Co;2-q, 2000.

Kjaergaard, H. G., Knap, H. C., Ørnsø, K. B., Jørgensen, S., Crounse, J. D., Paulot, F., and Wennberg, P. O.: Atmospheric fate of methacrolein. 2. Formation of lactone and implications for organic aerosol production, J Phys Chem A, 116, 5763-5768, 10.1021/jp210853h, 2012.

Kurokawa, J. and Ohara, T.: Long-term historical trends in air pollutant emissions in Asia: Regional Emission inventory in ASia (REAS) version 3, Atmos. Chem. Phys., 20, 12761-12793, 10.5194/acp-20-12761-2020, 2020.

Lewandowski, M., Piletic, I. R., Kleindienst, T. E., Offenberg, J. H., Beaver, M. R., Jaoui, M., Docherty, K. S., and Edney, E. O.: Secondary organic aerosol characterisation at field sites across the United States during the spring–summer period, Int J Environ Anal Chem, 93, 1084-1103, 10.1080/03067319.2013.803545, 2013.

Li, J., Xie, X., Li, L., Wang, X., Wang, H., Jing, S. a., Ying, Q., Qin, M., and Hu, J.: Fate of Oxygenated Volatile Organic Compounds in the Yangtze River Delta Region: Source Contributions and Impacts on the Atmospheric Oxidation Capacity, Environ Sci Technol, 56, 11212-11224, 10.1021/acs.est.2c00038, 2022.

Lin, Y. H., Knipping, E. M., Edgerton, E. S., Shaw, S. L., and Surratt, J. D.: Investigating the influences of $SO_2$ and $NH_3$ levels on isoprene-derived secondary organic aerosol formation using conditional sampling approaches, Atmos. Chem. Phys., 13, 8457-8470, 10.5194/acp-13-8457-2013, 2013a.

Lin, Y. H., Zhang, H., Pye, H. O. T., Zhang, Z., Marth, W. J., Park, S., Arashiro, M., Cui, T., Budisulistiorini, S. H., and Sexton, K. G.: Epoxide as a precursor to secondary organic aerosol formation from isoprene photooxidation in the presence of nitrogen oxides, Proc. Natl. Acad. Sci., 110, 6718-6723, 2013b.

Lin, Y. H., Zhang, Z. F., Docherty, K. S., Zhang, H. F., Budisulistiorini, S. H., Rubitschun, C. L., Shaw, S. L., Knipping, E. M., Edgerton, E. S., Kleindienst, T. E., Gold, A., and Surratt, J. D.: Isoprene Epoxydiols as Precursors to Secondary Organic Aerosol Formation: Acid-Catalyzed Reactive Uptake Studies with Authentic Compounds, Environ Sci Technol, 46, 250-258, 10.1021/es202554c, 2012.

Ling, Z., He, Z., Wang, Z., Shao, M., and Wang, X.: Sources of methacrolein and methyl vinyl ketone and their contributions to methylglyoxal and formaldehyde at a receptor site in Pearl River Delta, J. Environ. Sci., 79, 1-10, https://doi.org/10.1016/j.jes.2018.12.001, 2019.

https://doi.org/10.5194/egusphere-2025-1909
Preprint. Discussion started: 15 May 2025


738 Liu, Y., Yang, X., Tan, J., and Li, M.: Concentration prediction and spatial origin analysis of criteria air
739 pollutants in Shanghai, Environ. Pollut., 327, 121535, https://doi.org/10.1016/j.envpol.2023.121535,
740 2023a.

741 Liu, Y., Geng, G., Cheng, J., Liu, Y., Xiao, Q., Liu, L., Shi, Q., Tong, D., He, K., and Zhang, Q.: Drivers of
742 Increasing Ozone during the Two Phases of Clean Air Actions in China 2013-2020, Environ Sci Technol,
743 57, 10.1021/acs.est.3c00054, 2023b.

744 McNeill, V. F., Woo, J. L., Kim, D. D., Schwier, A. N., Wannell, N. J., Sumner, A. J., and Barakat, J. M.:
745 Aqueous-phase secondary organic aerosol and organosulfate formation in atmospheric aerosols: a
746 modeling study, Environ Sci Technol, 46 15, 8075-8081, 2012.

747 Nguyen, T. B., Bates, K. H., Crounse, J. D., Schwantes, R. H., Zhang, X., Kjaergaard, H. G., Surratt, J. D.,
748 Lin, P., Laskin, A., Seinfeld, J. H., and Wennberg, P. O.: Mechanism of the hydroxyl radical oxidation of
749 methacryloyl peroxynitrate (MPAN) and its pathway toward secondary organic aerosol formation in the
750 atmosphere, Phys. Chem. Chem. Phys., 17, 17914-17926, 10.1039/c5cp02001h, 2015.

751 Orlando, J. J., Tyndall, G. S., and Paulson, S. E.: Mechanism of the OH-initiated oxidation of methacrolein,
752 Geophys. Res. Lett, 26, 2191-2194, https://doi.org/10.1029/1999GL900453, 1999.

753 Park, C., Schade, G. W., and Boedeker, I.: Characteristics of the flux of isoprene and its oxidation products
754 in an urban area, J Geophys Res-atmos, 116, 10.1029/2011jd015856, 2011.

755 Paulot, F., Crounse, J. D., Kjaergaard, H. G., Kurten, A., St Clair, J. M., Seinfeld, J. H., and Wennberg, P. O.:
756 Unexpected Epoxide Formation in the Gas-Phase Photooxidation of Isoprene, Science, 325, 730-733,
757 10.1126/science.1172910, 2009.

758 Piletic, I. R., Edney, E. O., and Bartolotti, L. J.: A computational study of acid catalyzed aerosol reactions of
759 atmospherically relevant epoxides, Phys. Chem. Chem. Phys., 15, 18065-18076, 10.1039/c3cp52851k,
760 2013.

761 Pye, H. O. T., Pinder, R. W., Piletic, I. R., Xie, Y., Capps, S. L., Lin, Y.-H., Surratt, J. D., Zhang, Z., Gold,
762 A., Luecken, D. J., Hutzell, W. T., Jaoui, M., Offenberg, J. H., Kleindienst, T. E., Lewandowski, M., and
763 Edney, E. O.: Epoxide Pathways Improve Model Predictions of Isoprene Markers and Reveal Key Role
764 of Acidity in Aerosol Formation, Environ Sci Technol, 47, 11056-11064, 10.1021/es402106h, 2013.

765 Pye, H. O. T., Murphy, B. N., Xu, L., Ng, N. L., Carlton, A. G., Guo, H., Weber, R., Vasilakos, P., Appel, K.
766 W., Budisulistiorini, S. H., Surratt, J. D., Nenes, A., Hu, W., Jimenez, J. L., Isaacman-VanWertz, G.,
767 Misztal, P. K., and Goldstein, A. H.: On the implications of aerosol liquid water and phase separation for
768 organic aerosol mass, Atmos. Chem. Phys., 17, 343-369, 10.5194/acp-17-343-2017, 2017.

769 Qin, M., Wang, X., Hu, Y., Ding, X., Song, Y., Li, M., Vasilakos, P., Nenes, A., and Russell, A. G.: Simulating
770 Biogenic Secondary Organic Aerosol During Summertime in China, J Geophys Res-atmos, 123, 11,100-
771 111,119, https://doi.org/10.1029/2018JD029185, 2018.

772 Rattanavaraha, W., Chu, K., Budisulistiorini, S. H., Riva, M., Lin, Y. H., Edgerton, E. S., Baumann, K., Shaw,
773 S. L., Guo, H., King, L., Weber, R. J., Neff, M. E., Stone, E. A., Offenberg, J. H., Zhang, Z., Gold, A., and
774 Surratt, J. D.: Assessing the impact of anthropogenic pollution on isoprene-derived secondary organic
775 aerosol formation in $PM_{2.5}$ collected from the Birmingham, Alabama, ground site during the 2013
776 Southern Oxidant and Aerosol Study, Atmos. Chem. Phys., 16, 4897-4914, 10.5194/acp-16-4897-2016,
777 2016.

https://doi.org/10.5194/egusphere-2025-1909
Preprint. Discussion started: 15 May 2025


778 Riedel, T. P., Lin, Y. H., Zhang, Z., Chu, K., Thornton, J. A., Vizuete, W., Gold, A., and Surratt, J. D.:
779 Constraining condensed-phase formation kinetics of secondary organic aerosol components from isoprene
780 epoxydiols, Atmos. Chem. Phys., 16, 1245-1254, 10.5194/acp-16-1245-2016, 2016.

781 Riedel, T. P., Lin, Y.-H., Budisulistiorini, H., Gaston, C. J., Thornton, J. A., Zhang, Z., Vizuete, W., Gold, A.,
782 and Surrattt, J. D.: Heterogeneous Reactions of Isoprene-Derived Epoxides: Reaction Probabilities and
783 Molar Secondary Organic Aerosol Yield Estimates, Environ. Sci. Technol. Lett., 2, 38-42,
784 10.1021/ez500406f, 2015.

785 Schwantes, R. H., Teng, A. P., Nguyen, T. B., Coggon, M. M., Crounse, J. D., St. Clair, J. M., Zhang, X.,
786 Schilling, K. A., Seinfeld, J. H., and Wennberg, P. O.: Isoprene $NO_3$ Oxidation Products from the $RO_2$ +
787 $HO_2$ Pathway, J. Phys. Chem. A, 119, 10158-10171, 10.1021/acs.jpca.5b06355, 2015.

788 Shrivastava, M., Andreae, M. O., Artaxo, P., Barbosa, H. M. J., Berg, L. K., Brito, J., Ching, J., Easter, R. C.,
789 Fan, J., Fast, J. D., Feng, Z., Fuentes, J. D., Glasius, M., Goldstein, A. H., Alves, E. G., Gomes, H., Gu,
790 D., Guenther, A., Jathar, S. H., Kim, S., Liu, Y., Lou, S., Martin, S. T., McNeill, V. F., Medeiros, A., de Sa,
791 S. S., Shilling, J. E., Springston, S. R., Souza, R. A. F., Thornton, J. A., Isaacman-VanWertz, G., Yee, L.
792 D., Ynoue, R., Zaveri, R. A., Zelenyuk, A., and Zhao, C.: Urban pollution greatly enhances formation of
793 natural aerosols over the Amazon rainforest, Nat. Commun, 10, 10.1038/s41467-019-08909-4, 2019.

794 St. Clair, J. M., Rivera-Rios, J. C., Crounse, J. D., Knap, H. C., Bates, K. H., Teng, A. P., Jørgensen, S.,
795 Kjaergaard, H. G., Keutsch, F. N., and Wennberg, P. O.: Kinetics and Products of the Reaction of the First-
796 Generation Isoprene Hydroxy Hydroperoxide (ISOPOOH) with OH, J. Phys. Chem. A, 120, 1441-1451,
797 10.1021/acs.jpca.5b06532, 2016.

798 Stone, E. A., Nguyen, T. T., Pradhan, B. B., and Man Dangol, P.: Assessment of biogenic secondary organic
799 aerosol in the Himalayas, Environ. Chem. , 9, 263-272, https://doi.org/10.1071/EN12002, 2012.

800 Surratt, J. D., Chan, A., Eddingsaas, N. C., Chan, M. N., Loza, C. L., Kwan, A. J., Hersey, S. P., Flagan, R.
801 C., Wennberg, P. O., and Seinfeld, J. H.: Reactive intermediates revealed in secondary organic aerosol
802 formation from isoprene, Proc. Natl. Acad. Sci., 107, 6640-6645, 2010.

803 Surratt, J. D., Kroll, J. H., Kleindienst, T. E., Edney, E. O., Claeys, M., Sorooshian, A., Ng, N. L., Offenberg,
804 J. H., Lewandowski, M., Jaoui, M., Flagan, R. C., and Seinfeld, J. H.: Evidence for organosulfates in
805 secondary organic aerosol, Environ Sci Technol, 41, 517-527, 10.1021/es062081q, 2007.

806 Tao, S., Lu, X., Levac, N., Bateman, A. P., Nguyen, T. B., Bones, D. L., Nizkorodov, S. A., Laskin, J., Laskin,
807 A., and Yang, X.: Molecular Characterization of Organosulfates in Organic Aerosols from Shanghai and
808 Los Angeles Urban Areas by Nanospray-Desorption Electrospray Ionization High-Resolution Mass
809 Spectrometry, Environ Sci Technol, 48, 10993-11001, 10.1021/es5024674, 2014.

810 Teng, A. P., Crounse, J. D., and Wennberg, P. O.: Isoprene Peroxy Radical Dynamics, J.Am.Chem.Soc, 139,
811 5367-5377, 10.1021/jacs.6b12838, 2017.

812 Wang, H., Wang, H., Lu, X., Lu, K., Zhang, L., Tham, Y. J., Shi, Z., Aikin, K., Fan, S., Brown, S. S., and
813 Zhang, Y.: Increased night-time oxidation over China despite widespread decrease across the globe, Nat.
814 Geosci, 16, 217-223, 10.1038/s41561-022-01122-x, 2023a.

815 Wang, M., Duan, Y., Xu, W., Wang, Q., Zhang, Z., Yuan, Q., Li, X., Han, S., Tong, H., Huo, J., Chen, J., Gao,
816 S., Wu, Z., Cui, L., Huang, Y., Xiu, G., Cao, J., Fu, Q., and Lee, S.: Measurement report: Characterisation

https://doi.org/10.5194/egusphere-2025-1909
Preprint. Discussion started: 15 May 2025


and sources of the secondary organic carbon in a Chinese megacity over 5 years from 2016 to 2020, Atmos. Chem. Phys., 22, 12789-12802, 10.5194/acp-22-12789-2022, 2022.

Wang, W., Wu, M. H., Li, L., Zhang, T., Liu, X. D., Feng, J. L., Li, H. J., Wang, Y. J., Sheng, G. Y., Claeys, M., and Fu, J. M.: Polar organic tracers in $PM_{2.5}$ aerosols from forests in eastern China, Atmos. Chem. Phys., 8, 7507-7518, 10.5194/acp-8-7507-2008, 2008.

Wang, Y., Zhao, Y., Wang, Y., Yu, J.-Z., Shao, J., Liu, P., Zhu, W., Cheng, Z., Li, Z., Yan, N., and Xiao, H.: Organosulfates in atmospheric aerosols in Shanghai, China: seasonal and interannual variability, origin, and formation mechanisms, Atmos. Chem. Phys., 21, 2959-2980, 10.5194/acp-21-2959-2021, 2021.

Wang, Y., Zhang, Y., Li, W., Wu, G., Qi, Y., Li, S., Zhu, W., Yu, J. Z., Yu, X., Zhang, H.-H., Sun, J., Wang, W., Sheng, L., Yao, X., Gao, H., Huang, C., Ma, Y., and Zhou, Y.: Important Roles and Formation of Atmospheric Organosulfates in Marine Organic Aerosols: Influence of Phytoplankton Emissions and Anthropogenic Pollutants, Environ Sci Technol, 57, 10284-10294, 10.1021/acs.est.3c01422, 2023b.

Wiedinmyer, C., Kimura, Y., McDonald-Buller, E. C., Emmons, L. K., Buchholz, R. R., Tang, W., Seto, K., Joseph, M. B., Barsanti, K. C., Carlton, A. G., and Yokelson, R.: The Fire Inventory from NCAR version 2.5: an updated global fire emissions model for climate and chemistry applications, Geosci. Model Dev., 16, 3873-3891, 10.5194/gmd-16-3873-2023, 2023.

Worton, D. R., Surratt, J. D., LaFranchi, B. W., Chan, A. W. H., Zhao, Y., Weber, R. J., Park, J.-H., Gilman, J. B., de Gouw, J., Park, C., Schade, G., Beaver, M., St Clair, J. M., Crounse, J., Wennberg, P., Wolfe, G. M., Harrold, S., Thornton, J. A., Farmer, D. K., Docherty, K. S., Cubison, M. J., Jimenez, J.-L., Frossard, A. A., Russell, L. M., Kristensen, K., Glasius, M., Mao, J., Ren, X., Brune, W., Browne, E. C., Pusede, S. E., Cohen, R. C., Seinfeld, J. H., and Goldsteint, A. H.: Observational Insights into Aerosol Formation from Isoprene, Environ Sci Technol, 47, 11403-11413, 10.1021/es4011064, 2013.

Xu, L., Middlebrook, A. M., Liao, J., de Gouw, J. A., Guo, H., Weber, R. J., Nenes, A., Lopez-Hilfiker, F. D., Lee, B. H., Thornton, J. A., Brock, C. A., Neuman, J. A., Nowak, J. B., Pollack, I. B., Welti, A., Graus, M., Warneke, C., and Ng, N. L.: Enhanced formation of isoprene-derived organic aerosol in sulfur-rich power plant plumes during Southeast Nexus, J Geophys Res-atmos, 121, 11,137-111,153, https://doi.org/10.1002/2016JD025156, 2016.

Xu, L., Guo, H., Boyd, C. M., Klein, M., Bougiatioti, A., Cerully, K. M., Hite, J. R., Isaacman-VanWertz, G., Kreisberg, N. M., Knote, C., Olson, K., Koss, A., Goldstein, A. H., Hering, S. V., de Gouw, J., Baumann, K., Lee, S.-H., Nenes, A., Weber, R. J., and Ng, N. L.: Effects of anthropogenic emissions on aerosol formation from isoprene and monoterpenes in the southeastern United States, Proc. Natl. Acad. Sci., 112, 37-42, doi:10.1073/pnas.1417609112, 2015.

Yan, K., Wang, J., Peng, R., Yang, K., Chen, X., Yin, G., Dong, J., Weiss, M., Pu, J., and Myneni, R. B.: HiQ-LAI: a high-quality reprocessed MODIS leaf area index dataset with better spatiotemporal consistency from 2000 to 2022, Earth Syst. Sci. Data, 16, 1601-1622, 10.5194/essd-16-1601-2024, 2024.

Yao, Y., Wang, W., Ma, K., Tan, H., Zhang, Y., Fang, F., and He, C.: Transmission paths and source areas of near-surface ozone pollution in the Yangtze River delta region, China from 2015 to 2021, J. Environ. Manage., 330, 117105, https://doi.org/10.1016/j.jenvman.2022.117105, 2023.

https://doi.org/10.5194/egusphere-2025-1909
Preprint. Discussion started: 15 May 2025


Ye, J., Abbatt, J. P. D., and Chan, A. W. H.: Novel pathway of $SO_2$ oxidation in the atmosphere: reactions with monoterpene ozonolysis intermediates and secondary organic aerosol, Atmos. Chem. Phys., 18, 5549-5565, 10.5194/acp-18-5549-2018, 2018.

Yee, L. D., Isaacman-VanWertz, G., Wernis, R. A., Kreisberg, N. M., Glasius, M., Riva, M., Surratt, J. D., de Sá, S. S., Martin, S. T., Alexander, M. L., Palm, B. B., Hu, W., Campuzano-Jost, P., Day, D. A., Jimenez, J. L., Liu, Y., Misztal, P. K., Artaxo, P., Viegas, J., Manzi, A., de Souza, R. A. F., Edgerton, E. S., Baumann, K., and Goldstein, A. H.: Natural and Anthropogenically Influenced Isoprene Oxidation in Southeastern United States and Central Amazon, Environ Sci Technol, 54, 5980-5991, 10.1021/acs.est.0c00805, 2020.

Zang, H., Zhao, Y., Huo, J., Zhao, Q., Fu, Q., Duan, Y., Shao, J., Huang, C., An, J., Xue, L., Li, Z., Li, C., and Xiao, H.: High atmospheric oxidation capacity drives wintertime nitrate pollution in the eastern Yangtze River Delta of China, Atmos. Chem. Phys., 22, 4355-4374, 10.5194/acp-22-4355-2022, 2022.

Zhang, J., Liu, J., Ding, X., He, X., Zhang, T., Zheng, M., Choi, M., Isaacman-VanWertz, G., Yee, L., Zhang, H., Misztal, P., Goldstein, A. H., Guenther, A. B., Budisulistiorini, S. H., Surratt, J. D., Stone, E. A., Shrivastava, M., Wu, D., Yu, J. Z., and Ying, Q.: New formation and fate of Isoprene SOA markers revealed by field data-constrained modeling, npj Clim. Atmos. Sci., 6, 69, 10.1038/s41612-023-00394-3, 2023.

Zhang, Y.-Q., Chen, D.-H., Ding, X., Li, J., Zhang, T., Wang, J.-Q., Cheng, Q., Jiang, H., Song, W., Ou, Y.-B., Ye, P.-L., Zhang, G., and Wang, X.-M.: Impact of anthropogenic emissions on biogenic secondary organic aerosol: observation in the Pearl River Delta, southern China, Atmos. Chem. Phys., 19, 14403-14415, 10.5194/acp-19-14403-2019, 2019.

Zhang, Y.-Q., Ding, X., He, Q.-F., Wen, T.-X., Wang, J.-Q., Yang, K., Jiang, H., Cheng, Q., Liu, P., Wang, Z.-R., He, Y.-F., Hu, W.-W., Wang, Q.-Y., Xin, J.-Y., Wang, Y.-S., and Wang, X.-M.: Observational Insights into Isoprene Secondary Organic Aerosol Formation through the Epoxide Pathway at Three Urban Sites from Northern to Southern China, Environ Sci Technol, 10.1021/acs.est.1c06974, 2022.

Zhao, D., Schmitt, S. H., Wang, M., Acir, I.-H., Tillmann, R., Tan, Z., Novelli, A., Fuchs, H., Pullinen, I., Wegener, R., Rohrer, F., Wildt, J., Kiendler-Scharr, A., Wahner, A., and Mentel, T. F.: Effects of NOx and $SO_2$ on the secondary organic aerosol formation from photooxidation of α-pinene and limonene, Atmos. Chem. Phys., 18, 1611-1628, 10.5194/acp-18-1611-2018, 2018.

Zhao, M., Qiao, T., Huang, Z., Zhu, M., Xu, W., Xiu, G., Tao, J., and Lee, S.: Comparison of ionic and carbonaceous compositions of $PM_{2.5}$ in 2009 and 2012 in Shanghai, China, Sci Total Environ, 536, 695-703, 10.1016/j.scitotenv.2015.07.100, 2015.

Zhao, Z., Xu, Q., Yang, X., and Zhang, H.: Heterogeneous Ozonolysis of Endocyclic Unsaturated Organic Aerosol Proxies: Implications for Criegee Intermediate Dynamics and Later-Generation Reactions, ACS Earth Space Chem, 3, 344-356, 10.1021/acsearthspacechem.8b00177, 2019.

Zheng, B., Tong, D., Li, M., Liu, F., Hong, C., Geng, G., Li, H., Li, X., Peng, L., Qi, J., Yan, L., Zhang, Y., Zhao, H., Zheng, Y., He, K., and Zhang, Q.: Trends in China's anthropogenic emissions since 2010 as the consequence of clean air actions, Atmos. Chem. Phys., 18, 14095-14111, 10.5194/acp-18-14095-2018, 2018.

https://doi.org/10.5194/egusphere-2025-1909
Preprint. Discussion started: 15 May 2025


893 Zhong, Y., Chen, J., Zhao, Q., Zhang, N., Feng, J., and Fu, Q.: Temporal trends of the concentration and
894 sources of secondary organic aerosols in $PM_{2.5}$ in Shanghai during 2012 and 2018, Atmos. Environ, 261,
895 118596, https://doi.org/10.1016/j.atmosenv.2021.118596, 2021.
896 Zhou, M., Zheng, G., Wang, H., Qiao, L., Zhu, S., Huang, D., An, J., Lou, S., Tao, S., Wang, Q., Yan, R.,
897 Ma, Y., Chen, C., Cheng, Y., Su, H., and Huang, C.: Long-term trends and drivers of aerosol pH in eastern
898 China, Atmos. Chem. Phys., 22, 13833-13844, 10.5194/acp-22-13833-2022, 2022.
899